2016

Time-resolved photoluminescence studies of point defects in GaN

Joy Dorene McNamara
Virginia Commonwealth University

Time-resolved Photoluminescence Studies of Point Defects in GaN

A Dissertation submitted in partial fulfillment of the requirements for the degree of Doctor of Philosophy in Nanoscience and Nanotechnology at Virginia Commonwealth University.

By:

Joy Dorene McNamara

M.S. Applied Physics, Virginia Commonwealth University, 2013

B.S. Physics, Virginia Commonwealth University, 2011

Director:

Dr. Michael A. Reshchikov

Associate Professor, Department of Physics

Virginia Commonwealth University

Richmond, Virginia 23284, USA

April 27, 2016

"Your degree is just the door. Your work ethic is the key, but it is only by the grace and the strength of God that you will walk through that door and help whoever may be on the other side."

- Stefan Vandenkooy [1]

In loving memory of Grandma Dorene McNamara
August 26, 1926 – April 17, 2016

Acknowledgments

The famous words, “No man is an island” were penned in 1624 by the English poet John Donne. No great achievement stands alone and this work is no exception.

The completion of this dissertation and research was made possible by the guidance, direction, and wisdom of my extremely competent advisor Dr. Michael Reshchikov, and to him I owe an enormous debt of gratitude. Thank you, Dr. Reshchikov, for the innumerous hours of teaching and training in your lab and for being willing and able to guide me in my scientific development for the past 5 years. I have learned how to think critically and analyze data effectively because of your example. Thank you for showing me how to be a “good” scientist.

The path of my physics career has ever been meticulously guided by the advice and example of Dr. Alison Baski. The mentorship I have received from you, Dr. Baski, is priceless. Ever since my first class with you in freshman Physics 207, I have been astounded by your knowledge, the application of such, and your lucid thought process. You have inspired me in multiple aspects of my scientific development, and imprinted on me your example of hard work, determination, skill, knowledge and perseverance. Thank you for inspiring me to be a strong and capable woman in science.

My first steps in the VCU Physics Department were guided by Janice Guyer and Evelyn Perham who nurtured and encouraged me every year. I am thankful for your impact on my life. To my friends in the VCU Physics department: Nahla, Karen, Mike, Anita, Lauren, Chris, Kenny, Kevin, Dalton, Amy, Daniel, Ibrahima, and Anthony. Together, we have overcome multiple obstacles, struggled through classes and exams, collaborated on research projects, and shared life as graduate students. I would not have made it this far without your friendship.

I am thankful for the support and kindness of my church family and for each person who prayed me through these long nine years of school. Thank you to Rebecca Saunders for lunch dates, phone calls and for always being there; to Kelly and Keith Ober for the multitude of prayers and encouragement to keep my eyes on Jesus and to press on; to Rebecca Woods for cheering me on; to Betsy Smith for consistent prayers; to Barry and Nancy Gilman, Nick Pugh, and Gloria Duffey for every kind word and hug; to my sweet friends, Cristy, Stephanie, Sarah T., Kristina, Katie, and Kathleen, for your priceless friendship and constant prayers; and to my two besties, “Drs.” Olivia Gad and Reena Thomas who fill my life with love, laughter and many memorable moments.

Finally, to the ones who deserve the most credit for their laudable sacrifice: my mother, for always being there for me every day and night, for encouraging me, cheering me on, praying for me and filling my heart with kind words; and to my father, for instilling in me a love for

science, for helping me with homework and research and for inspiring me to be a life-long learner. Truly, they deserve the most praise for their constant support of me during this time. To Joel and Daniel, my best friends, for your support, companionship, and encouragement. Thanks for the numerous outings and moral building moments, for being there for me this whole time. I could not have done it without you. To my brothers David and Peter: thank you for your support, constant life advice and for being an example of hard work and discipline. I have been trying to follow in your footsteps this whole time. To my sisters Ruthie, Mary and Muy – beautiful, talented, godly, intelligent and such hard-working ladies. Thank you for your kindness and support during this time and for filling my life with many fun adventures.

Last, but not least, these words are for my nieces, Lily and Poppy, and for my cousin Jordyn Jane. Think more often than you feel. Treat yourself with dignity and respect, and only be close to those who give that to you. Remember that your identity cannot be changed by anyone around you. Your brain is just as beautiful as your outward appearance, so try to give both equal attention. Dream big dreams and challenge yourself to go further than you thought you could. Acknowledge God every step of your life, and He will direct your paths down ways you never dreamed possible.

All glory to God who created me with life, breath, and ability, and who gifted me with physical stamina, the capability to work and an insatiable desire to learn about the complexities of physics. Without the strength of God fueling my actions, my feeble efforts would have been in vain. This degree is for you, Jesus!

Table of Contents

Table of Figures (captions)

Abstract

TIME-RESOLVED PHOTOLUMINESCENCE STUDIES OF POINT DEFECTS IN GaN

Joy Dorene McNamara
Doctor of Philosophy in Nanoscience and Nanotechnology

A Dissertation submitted in partial fulfillment of the requirements for the degree of Doctor of Philosophy in Nanoscience & Nanotechnology at Virginia Commonwealth University.

Virginia Commonwealth University
2016

Major Director:
Dr. Michael A. Reshchikov
Associate Professor, Department of Physics

Time-resolved photoluminescence (TRPL) measurements paired with steady-state photoluminescence (SSPL) measurements can help to determine the PL lifetime, shape and position of unresolved bands, capture coefficients, and concentrations of free electrons and defects. PL bands that are obscured in the SSPL spectra can be accurately revealed by TRPL measurements. TRPL measurements are able to show if the PL band originates from an internal transition between different states of the same defect. The main defect-related PL bands in high-purity GaN grown by hydride vapor phase epitaxy (HVPE) which have been investigated are the

ultraviolet, blue, green, yellow and red luminescence bands (UVL, BL, GL, YL and RL, respectively). The concentration of free electrons can be calculated from these measurements providing a contactless alternative to the Hall effect method. The lifetime of most defect-related PL bands decreases with increasing temperature. However, the lifetime of the GL band, with a maximum at 2.4 eV observed in the SSPL spectra only at high excitation intensity, increases as a function of temperature. By analyzing the PL intensity decay, the origin of the GL can be attributed to an internal transition from an excited state of the C_N defect, which behaves as an optically generated giant trap, to the 0/+ level of the same defect. This first observation of an optically generated giant trap was detected by analyzing the cubic temperature dependence of the electron capture coefficient. Excitation intensity and temperature dependent studies on Mg-doped GaN grown by HVPE were performed. The position of the UVL (3.2 eV) peak blue-shifts with increasing excitation intensity, which can be explained by the presence of potential fluctuations. The BL peak (2.8 eV) also blue-shifts with increasing excitation intensity, and red-shifts as a function of temperature. These shifts can be explained by the transitions originating from a deep-donor to the Mg_{Ga} acceptor, and the corresponding donor-acceptor pair nature.

Common Abbreviations

ATQ: abrupt and tunable quenching

BL: blue luminescence

CC: configuration coordinate

DAP: donor-acceptor pair

eA: free-to-bound electronic transitions

GaN: gallium nitride

GL: green luminescence

HVPE: hydride vapor phase epitaxy

IQE: internal quantum efficiency

MOCVD: metal organic chemical vapor deposition

PL: photoluminescence

RL: red luminescence

SSPL: steady-state photoluminescence

TRPL: time-resolved photoluminescence

UV: ultraviolet

UVL: ultraviolet luminescence

YL: yellow luminescence

ZPL: zero-phonon line

Chapter 1: An Introduction to GaN and Photoluminescence

1.1 Motivation to investigate GaN materials

Inasmuch as many have set about to compile information on the discoveries and understanding of gallium nitride (GaN) materials, it is fitting to compose an orderly account of the new understanding that has been acquired on the properties of point defects by steady state and time-resolved photoluminescence methods.

GaN has a wide-bandgap of 3.50 eV at 2 K [2] and is quickly gaining momentum as an ideal material for numerous applications and for valid reasons. It has achieved this success partly because of its "high" properties – high brightness, high frequency, high voltage, high temperature, high efficiency, and many more. LED's which use GaN as a base are known for their high brightness, and can emit light in the entire visible range by varying the composition of Al (AlGaN) and In (InGaN) and tuning the bandgap of the compound. Devices using GaN are able to withstand high voltages, very fast switching frequency, and have higher energy efficiencies as a result. Even more so, the wide bandgap of GaN leads to high heat capacity and the ability to withstand operation at comparatively high temperatures without thermal excitation affecting the performance of the device. The wide bandgap of GaN allows it to be very useful for visible short wavelength emitters and ultraviolet (UV) range detectors. The applications for this material seem endless as the list continues with optoelectronics, spintronics, low sensitivity to ionizing radiation for space usage, and long-operational-lifetime violet laser diodes. While GaN-

based materials may seem to be the answer to many energy- and lighting-related problems, the base understanding of GaN and the performance thereof has far to go. Specifically, defects in GaN contribute to the failure of devices and to the low efficiency of emitters, and the effect of such is surprisingly not well-understood.

Defects create undesirable channels of nonradiative recombination and lower the quantum efficiency. Defects may be intentionally and un-intentionally introduced, and can be classified into two broad categories: extended and point. Extended defects are those which spatially span much greater distances and include dislocations, clusters, grain boundaries, voids, surfaces and interfaces. Point defects are defects in the crystal lattice and the size of such is on the order of atomic distances. These include vacancies, interstitials, antisites, substitutional impurities, and complexes. Impurities, which are intentionally or unintentionally introduced, may be found as substitutionary or interstitial atoms. A substitutionary Mg acceptor in a Ga site, for example, is labeled Mg_{Ga} and interstitial hydrogen is labeled H_i. Native defects occur within the host material and are vacancies (labeled V_{Ga} or V_N), interstitial atoms, or antisites (such as Ga_N: a Ga atom in a N site). Finally, complexes composed of any combination of native defects and impurities may exist within the crystal lattice (e.g., C_NO_N complex) and are also considered as point defects. The primary focus of this work is on point defects, since a more comprehensive understanding of the nature, origin and properties of point defects is necessary in order for devices and applications of GaN to ultimately perform at higher levels and achieve higher efficiencies.

The GaN samples investigated in this work are grown by hydride (halide) vapor phase epitaxy (HVPE) and metal-organic chemical vapor deposition (MOCVD) and are freestanding layers or are deposited on sapphire substrates. For the purpose of obtaining *n*- or *p*-type

conductivity, which is necessary for diode-based devices, GaN is intentionally doped using elements such as Si (*n*-type) and Mg (*p*-type).

1.2 Photoluminescence

Photoluminescence (PL) is the spontaneous emission of photons from a semiconductor material after electrons in the material are excited by an energy source, such as a laser or lamp. Above-bandgap excitation creates an electron-hole pair in the conduction band and valence band, respectively, and resonant excitation excites an electron from a defect level in the bandgap to the conduction band or an electron from the valence band to a defect level. PL is observed when an excited electron recombines with a hole in a lower energy state. The energy of the emitted photon depends on the difference in energies of the electronic transition and the strength of the electron-phonon coupling.

Conventional methods of PL have been used for decades to understand the properties of GaN. Specifically, PL spectra provide information on the quality of the material and point to the specific origin and nature of the electronic transitions. In particular, we employ two versions of PL measurements: time-resolved photoluminescence (TRPL) excited with a N-pulse laser ($\hbar\omega$ = 3.68 eV), and steady-state photoluminescence (SSPL) excited using a HeCd laser ($\hbar\omega$ = 3.81 eV).

In SSPL, the laser continuously generates electron-hole pairs in the active region of the GaN layer which then recombine through both radiative and nonradiative channels. A monochromator analyzes the energies of PL produced by the sample, and the PL intensity is plotted as a function of photon energy. The PL spectra reveal information regarding the excitonic emission and defect-related emission. Analysis of these PL bands provides very useful

information for determining the properties of defects and the absolute internal quantum efficiency (IQE). Additional information can be garnered by varying the sample temperature and excitation intensity of the laser. To date, vast amounts of data have been gathered from SSPL measurements, and have provided valuable information on the identity and properties of defects to both theorists and experimentalists. However, in many samples, various defect-related PL bands overlap and are difficult to differentiate in terms of the shape, maximum, and zero-phonon line. The origin of many defect-related bands is still unknown, and fully understanding SSPL measurements is limited to spectra with clearly defined or well-known bands.

TRPL measurements, which use pulsed excitation to measure the PL intensity decay as a function of time, provide unique information on defect-related PL bands in conjunction with data obtained from SSPL measurements. Since bands with different origins will decay at different rates, TRPL provides a useful method for resolving overlapping PL bands. TRPL measurements can be performed as the sample temperature is varied or the excitation intensity of the laser is attenuated for a wide range of intensities. A variety of defect parameters can be calculated from TRPL data, and together with parameters obtained from SSPL, can unveil information regarding defect-related PL which has previously been unknown. The theory for modeling the spectra acquired from SSPL and TRPL is well-developed and can calculate the essential parameters needed to determine the identity of the defect.

1.3 Photoluminescence setup

Steady-state PL is excited by a continuous wave, He-Cd laser (40 mW, $\hbar\omega$ = 3.81 eV). The emitted PL is dispersed by a 1200 rules/ mm grating in a 0.3 m monochromator, then detected by a chilled photomultiplier tube. The intensity of the PL, P_{exc}, can be attenuated by

using neutral density filters with an unfocused laser beam (dia. = 4 mm). The range of excitation intensities can be varied between 2×10^{-7} to 0.2 W/cm^2. If the laser beam is focused to 0.1-0.2 mm, then intensities can reach 200 W/cm^2. A closed-cycle optical cryostat and a high-temperature cryostat both from Janis Research Co. are used to study PL in the range of 13 – 330 K and 100 – 650 K, respectively. A diagram of the experimental setup is shown in FIG. 1.1.

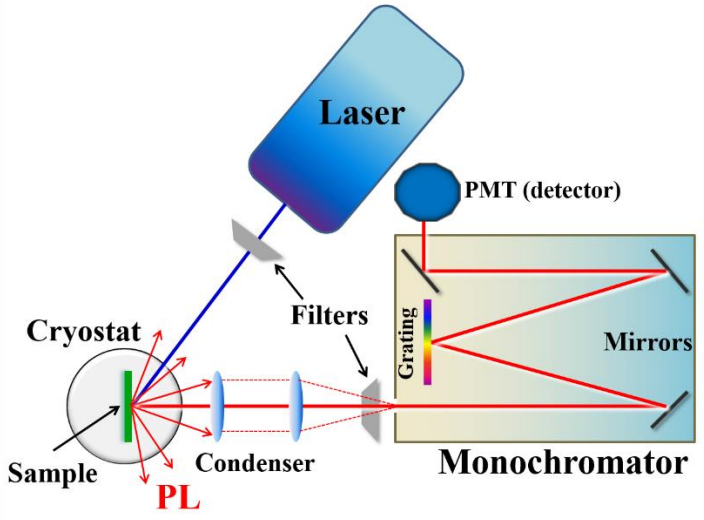

FIG. 1.1: A diagram of the components of the PL system.

A useful parameter of a particular PL band is the absolute IQE, η. As is shown in previous works, [3,4] the absolute IQE is defined as $\eta = I^{PL}/G$, where I^{PL} is the integrated PL intensity from a particular PL band and G is the concentration of electron-hole pairs created by the laser per second in the same volume. To find η for a particular PL band, we compared its integrated intensity with the PL intensity obtained from a calibrated GaN sample.

Time-resolved PL is excited using a nitrogen pulse laser, with $\hbar\omega$ = 3.68 eV, and the 1 ns pulses occurring with a frequency of 6 Hz. PL decay is analyzed using an oscilloscope, and the samples are mounted in the same cryostats as in the SSPL measurements to study the TRPL for a

wide range of temperatures. Each PL spectrum is corrected for the optical response of the system by comparing the spectra with the standard spectrum of a tungsten lamp.

Chapter 2: Theory and Models of Photoluminescence

2.1 Steady-state photoluminescence

A light source which emits above bandgap light can be used to excite PL in semiconductors. A laser can be used to generate a continuous number of electron-hole (e-h) pairs per unit volume, per second, and this rate is defined as *G*. Carrier dynamics and recombination behavior are greatly dependent on temperature, the concentration of free electrons, *n*, and holes, *p*, and on the concentration of donors, N_D, and acceptors, N_A, within the bandgap. [5] Typical electronic transitions within the bandgap are shown in FIG. 2.1. The generation of electron-hole pairs after the sample is illuminated with above-bandgap light is indicated by an upwards arrow. Recombinations of these pairs may occur from the conduction band to the valence band, which are so-called band-to-band transitions. Alternatively, excitons may be formed, and after annihilation will produce PL emission equal to the bandgap minus the binding energy of the excitons (~ 25 meV for GaN).[5] The topic of excitons is well-studied and is mostly beyond the scope of this work.

Defect-related emission usually occurs due to electronic transitions between the conduction band and defect levels, or directly between defect levels. At low temperatures and under illumination, electrons are quickly captured by positively charged donors and holes are captured by negatively charged acceptors. Defect-related emission at low temperature is mostly a

result of electrons transitioning from shallow donors to acceptors, called donor-acceptor pair (DAP) transitions.

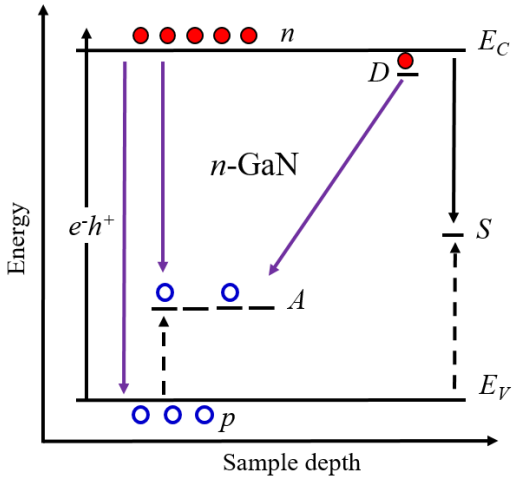

FIG. 2.1: Diagram of electronic transitions in GaN with a bandgap, E_g = 3.50 eV. Electron-hole pairs (e^-h^+) are created by above bandgap light, and recombine through various channels. Labels are as follows: acceptor level, *A*, donor level, *D*, non-radiative defect, *S*, conduction band minimum, E_C, valence band maximum, E_V, free electrons, *n*, and free holes, *p*.

Transitions involving deep donors in *n*-type semiconductors are less likely to contribute to the PL spectrum because acceptors usually capture photo-generated holes much more efficiently than donors, if the concentrations of deep donors and competing acceptors are comparable. As the temperature increases, sufficient thermal energy is supplied to ionize the shallow donors, and recombination then occurs mostly from the conduction band to acceptors (*eA* transitions). A further increase in temperature will ionize the acceptors. When holes are ionized from a particular acceptor, this recombination channel is said to be quenched, in that the intensity of PL from the acceptor will decrease as a function of increasing temperature. The ionized holes will be redistributed to other channels of recombination which may include the same acceptors or other deeper radiative and non-radiative channels, with concentration N_S.

An example of PL spectra for undoped GaN taken at T = 20 K is shown in FIG. 2.2. The defect related emission begins with the ultraviolet luminescence (UVL) band with the main peak

at 3.26 eV and the phonon replicas at 91 meV away from the main peak. In this spectra, blue luminescence (BL), yellow luminescence (YL), and red luminescence (RL) are also present with the main peak of the BL band found at 2.9 eV, 2.2 eV for the YL band, and the maximum of the RL band residing at 1.8 eV.

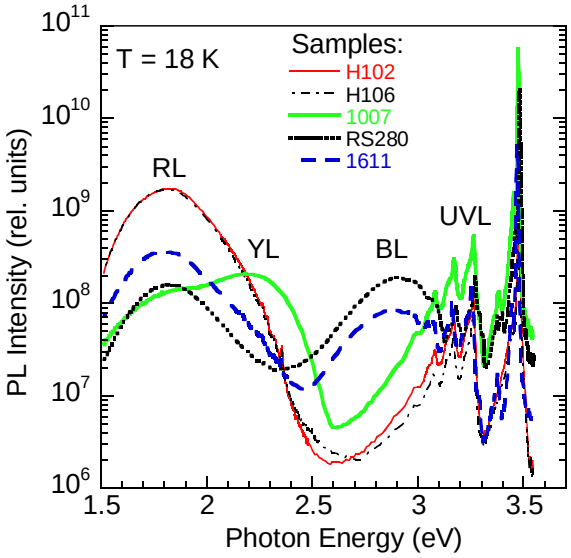

FIG. 2.2: PL spectra of several undoped, HVPE GaN measured at T = 18 K. The defect-related PL peaks of the UVL, BL and RL bands are as labeled. [6]

Numerous defect-related bands can be observed in GaN, depending on growth conditions of the layers, polarity, doping levels, and the concentrations of impurities. FIG. 2.3 gives an example of observed PL bands in undoped GaN and FIG. 2.4 gives theoretical predictions for the transitions which are responsible for PL.

With increasing temperature, the PL intensity decreases which is called the PL quenching. The slope of the temperature dependence plotted in a form of Arrhenius plot often reveals the activation energy of the related defect. If the quenching of a particular band occurs within a small range of temperatures and with a change in the PL intensity of a few orders of magnitude, the quenching is said to be abrupt and tunable quenching (ATQ).[3]

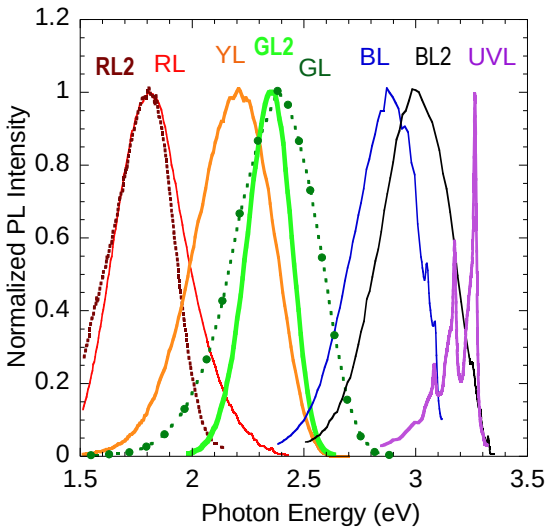

FIG. 2.3: Normalized PL spectra representing the most common defect-related bands observed in undoped GaN at T = 18 K.[7]

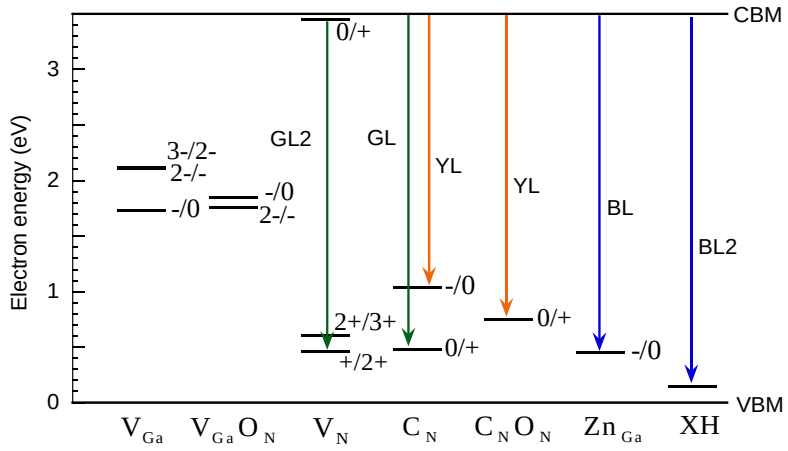

FIG. 2.4: Theoretical predictions of the PL transitions in undoped GaN. Thermodynamic transitions are expected to correspond to the zero-phonon lines, and are shown with horizontal bars. Vertical arrows indicate optical transitions and their correspondence to the observed PL bands in GaN. Transitions via the V_{Ga} and $V_{Ga}O_N$ defects are most likely nonradiative. The XH center may be the $C_NO_NH_i$ or C_NH_i complex.[8]

This is caused by ionized holes from the acceptors being captured by deep nonradiative defects, thereby redirecting the radiative recombination to nonradiative channels. The excitation intensity of the laser used for PL measurements can be attenuated by many orders of magnitude by using neutral density filters. At low excitation intensities, the dependence of PL intensity on the excitation intensity is linear for most defects. At higher excitation intensities, the defects become

saturated with photo-generated holes, and the quantum efficiency of the channel will reach saturation.

A. Rate equations of PL

Simple rate equations of the carrier dynamics under continuous illumination can be used to model the data obtained from PL spectra. To begin our consideration, we assume an *n*-type semiconductor with a concentration of donors, N_D, with ionization energy of E_D. In dark, there are free electrons with concentration n_0, and acceptors, N_A, with ionization energy E_A, are completely filled with electrons below the Fermi level. Of course, there are no free holes, p_0, in dark, in a wide-bandgap *n*-type semiconductor. Under illumination, a steady state concentration of free holes, δp, and free electrons, δn, is created by the laser with a generation rate G ($cm^{-3}s^{-1}$), in the volume of active PL per second. In the simplest approximation, we assume that G is constant within this volume, for the thickness α^{-1}, where α is the absorption coefficient, and G = 0 beyond this region of absorption. The total concentrations of free electrons and holes under any condition are given as n and p, respectively.

To describe the dynamics of electron-hole capture and recombination, we express the rate of transition as the product of the concentration of free charge carriers, the concentration of available empty sites and the capture coefficient of the given defect. [9,10] This provides a rate expression which can be used to describe the overall dynamics of the change in concentration of ionized defects of the free carriers. If C_{pA} is the hole capture coefficient for an acceptor, and C_{nA} is the electron capture coefficient for the same acceptor, then the term $C_{pA}N_A^- p$ describes the capture rate of holes by negatively charged acceptors, and the term $C_{nA}N_A^0 n$ describes the rate of recombination of electrons with holes bound to neutral acceptors.

The IQE of PL describes how efficiently the energy supplied by the laser is used to create radiative emission. The quantum efficiency can be experimentally determined by integrating the intensity of a particular PL band and normalizing by the excitation intensity of the laser. The intensity of PL through a given acceptor (if we ignore DAP transitions which is justified for $T > 100$ K) is given as,[11]

$$I^{PL} = C_{nA} N_A^0 n = \frac{N_A^0}{\tau_0}. \tag{2.1}$$

and the IQE is defined as,

$$\eta = \frac{I^{PL}}{G} = \frac{N_A^0}{\tau_0 G}, \tag{2.2}$$

where I^{PL} is the PL intensity integrated over the region of the given PL band, and the PL lifetime, τ_0, in the limit of low temperatures is defined from Eq. (2.1) as,

$$\tau_0 = (C_{nA} n)^{-1}. \tag{2.3}$$

We may go further to describe the change in concentration of holes bound to the acceptor during the process of e-h recombination:[11]

$$\frac{dN_A^0}{dt} = C_{pA} N_A^- p - C_{nA} N_A^0 n - Q_A N_A^0. \tag{2.4}$$

This expression includes the capture of free holes by negatively charged acceptors (first term on the right), and the recombination of electrons by the acceptor (second term on the right) which creates PL. In the third term on the right, we introduce a new parameter to describe the frequency of holes being thermally emitted to the valence band, which is defined as,

$$Q_A = C_{pA} N_v g^{-1} \exp\left(-\frac{E_A}{kT}\right) \tag{2.5}$$

where N_v is the effective density of states in the valence band, g is the degeneracy of the acceptor level (considered to be 2 for GaN), T is the temperature, and k is Boltzmann's constant. Finally, the temperature dependence of the PL IQE, η_A, through the acceptor is described as,[11]

$$\eta_A(T) = \frac{\eta_0}{1+(1-\eta_0)\tau_0 Q_A}. \tag{2.6}$$

with η_0 being the quantum efficiency in the limit of low temperature.

Equations (2.1)-(2.6) can be used as the basis for modeling the behavior of the PL as a function of temperature or excitation intensity. By fitting the temperature and excitation intensity dependences, the ionization energy of the acceptor can be determined either from the standard theory of PL quenching,[12] or from the theory of ATQ.[3]

B. Configuration coordinate diagrams for PL

The total energy of the defect system in its excited and ground state can be represented by a one-dimensional configuration coordinate (CC) diagram, in which the potential energy is represented by parabolas resembling the quantum harmonic oscillator. Two key concepts are the adiabatic approximation and the harmonic approximation. Since the mass of the electron is much smaller than the mass of the atom, their motions can be considered independently. This concept is the adiabatic approximation. The harmonic approximation is that the potential energy as a function of atom displacement, $V(x)$ is given as,

$$V(x) = (x - x_0)^2. \tag{2.7}$$

The CC diagram in its ground state is shown in FIG. 2.5 and represents the total energy of the defect system, including the electron and nuclear energies, and the screening potential of the surrounding atoms.[13,14,15,16,17,18]

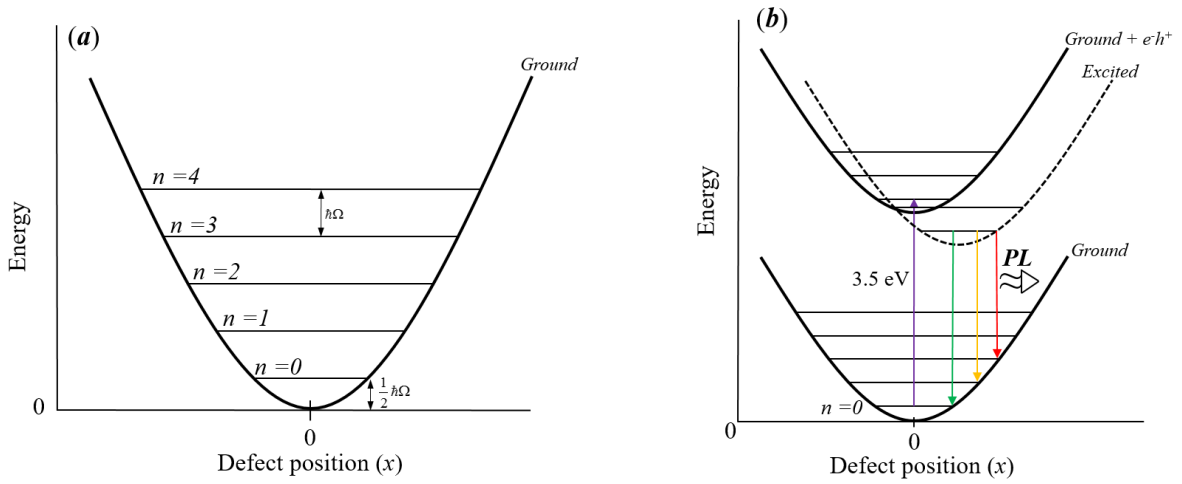

FIG. 2.5: Configuration coordinate diagram of defect system in (**a**) the ground state energy and equilibrium position, and (**b**) after excitation with 3.5 eV above bandgap light (labeled "*Ground* + e^-h^+"), capture of hole by the defect (labeled "*Excited*"), and radiative recombination of an electron with the hole at the defect to produce PL.

The position of the system is represented by a generalized coordinate *x*, since displacement can occur in a multitude of directions. The wave-function of the defect determines where the atom may be found at a certain time. The lowest energy state is represented by $n = 0$ in FIG. 2.5(a) , and higher energy levels are sequentially shown with equal spacing between the levels given by the quantity $\hbar\Omega$, the characteristic phonon energy of the defect, while the level $n = 0$ is half this quantity from the bottom of the parabola. If energy is supplied to the system through the form of above bandgap light, the total energy of the system will be represented by a second parabola shifted upwards by the amount of energy of the incident light, as shown in FIG. 2.5(b). This is representative of the energy of the defect system plus the energy of the electron hole pair. When a free hole is captured by the defect, the parabolas shift down in energy and also laterally as the center of mass for the defect oscillates about a new equilibrium to compensate for the change in electronic bonds and charges. The oscillations of the defect are in the form of lattice phonons and are quantized in units of $\hbar\Omega$. Phonon emission by the defect will be necessarily non-radiative. After the hole is captured by the defect, an electron from the

conduction band may recombine with it, causing the parabolas to shift down in energy for the radiative transitions and laterally to compensate for any phonons which are emitted non-radiatively. FIG. 2.5(b) shows the respective transitions and the expected PL energies based on the position of the defect at recombination and thus the number of phonons emitted. If the electron transitions from the zero-level state to zero-level state of two parabolas, no phonons are emitted and the respective PL transition will be the zero phonon line (ZPL) corresponding to the thermodynamic transition level.

Another interesting feature of CC diagrams is that they are capable of predicting the shape of a given PL band in the spectra based on the position of the PL maximum, the ZPL, and the average number of phonons emitted. An expression can be derived from these models to analyze the shape of a PL band in the spectrum and is given as[19]

$$I^{PL}(\hbar\omega) = I^{PL}_{\max} \exp\left[-2S_e\left(\sqrt{\frac{E_0^* - \hbar\omega}{E_0^* - \hbar\omega_{\max}}} - 1\right)^2\right] \tag{2.8}$$

where $I^{PL}_{\max}$ is the intensity of the PL band maximum, $\hbar\omega_{\max}$ is the position of the PL band maximum, $\hbar\omega$ is the photon energy, $E_0^* = E_0 + 0.5\hbar\Omega_e$ and E_0 is the ZPL which is occasionally, experimentally observed, $\hbar\Omega_e$ is the effective phonon energy of the defect, and S_e is the Huang-Rhys factor, both in the excited state of the defect. To fit the shape of the PL band obtained in TRPL spectra, it is necessary to fit only the E_0^* and S_e parameters. Once this information is obtained concerning the shape and position of a given defect related PL band, this knowledge can be used to resolve other bands in PL spectra where the bands overlap. FIG. 2.6 shows an example of the YL band in Si-doped GaN which can be clearly resolved in the PL spectrum and thus fit using Eq. (2.8).

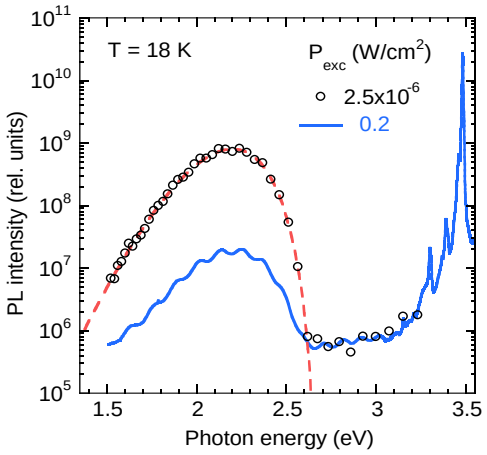

FIG. 2.6: The YL band in Si-doped GaN sample cvd3540 measured at T = 18 K for excitation intensities 2.5×10^{-6} and 0.2 W/cm^2. The shape of the YL band can be fit with Eq.(2.8), and the parameters S_e =7.4, $\hbar\omega_{max}$ = 2.20 eV, and E_0^* = 2.62 eV.

2.2 Time-resolved photoluminescence: measured lifetime of PL

The concept of PL lifetime is the "waiting" time for an electron to recombine radiatively with a hole. During the laser pulse (t_L ~1 ns), a burst of e-h pairs is created in an n-type semiconductor, and the photo-generated holes escape from the valence band after a short time delay (form excitons or are captured by defects). Given an ensemble of neutral acceptors, recombination may occur through any of these acceptors at any given instant in time. The PL intensity will begin to decay after the pulse, as the number of neutral acceptors decreases with time, slowing the e-h recombination. FIG. 2.7 shows the decay in time of PL intensity after a laser pulse, for the YL band for T = 18 and 300 K. The decay of the PL intensity in time for electron transitions from the conduction band to acceptors is given by the expression:

$$I^{PL}(t) = I^{PL}(0)\exp\left(\frac{-t}{\tau}\right). \qquad (2.9)$$

$I^{PL}(0)$ is the initial value of the PL intensity and τ is the measured PL lifetime. The effective lifetime of PL can be defined as the maximum of the function $I^{PL}(t)\times t$, where $I^{PL}(t)$ is the intensity of the PL decay at time t.[11] This is shown in FIG. 2.8 for the UVL band in HVPE GaN

sample H201, for the temperatures 60, 80, 100 and 120 K. The lifetime of PL decreases with increasing temperature since the concentration of free electrons increases with temperature.

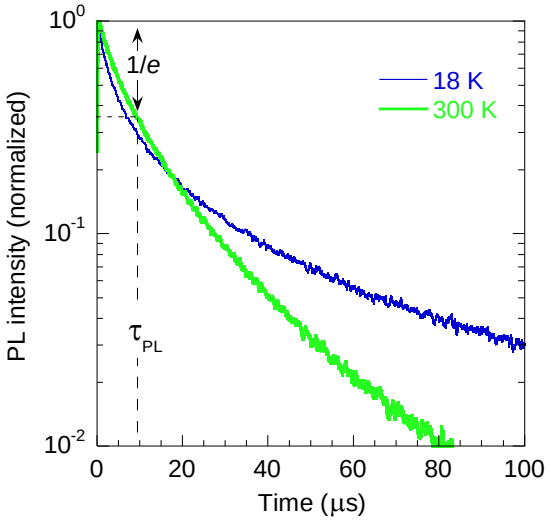

FIG. 2.7: Decay of the PL intensity detected at 560 nm after a laser pulse, for T = 18 and 300 K. The lifetime of PL, τ_{PL} , is the point in time where the PL intensity has decayed to the value of 1/e.

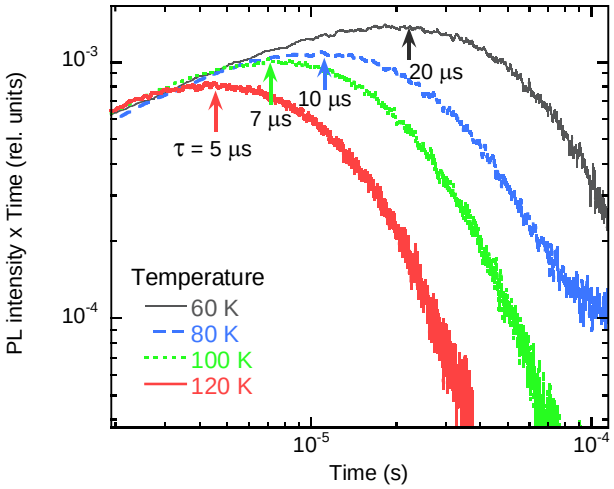

FIG. 2.8: Product of the PL intensity and time for the UVL decay (378 nm), for T = 60, 80, 100, and 120 K. The lifetime of PL, τ , is the maximum of the function, as indicated by the arrows on the figure.

Alternatively, we can describe the PL lifetime using well-known exponential decay relationships, such as those which are used to describe radioactive decay. The change in the concentration of neutral acceptors in time can be written as,

$$\frac{dN_A^0}{dt} = -\lambda N_A^0, \tag{2.10}$$

where N_A^0 is the concentration of neutral acceptors, and λ is the proportionality constant which can be determined by using an exponential solution of the form,

$$N_A^0 = N(0)\mathrm{e}^{\frac{-t}{\tau}}. \tag{2.11}$$

Solving Eq. (2.10) shows that,

$$\frac{dN_A^0}{dt} = -\frac{N_A^0}{\tau}. \tag{2.12}$$

In Section 2.1, an expression for the change in the concentration of neutral acceptors over time was derived to describe the phenomena of thermal quenching. Taking a closer look at Eq. (2.4), we can determine the value of τ by rearranging the expression to include what was derived in Eq. (2.12):

$$\frac{dN_A^0}{dt} = -\frac{N_A^0}{\tau} = -C_{nA}N_A^0 n - Q_A N_A^0 \tag{2.13}$$

The first term on the right in Eq. (2.4) is related to the capture of holes by negatively charged acceptors after the laser pulse. Since this capture time is very fast at low temperature (~10^{-10} s), we neglect this term for now, and write Eq. (2.13) as it is. The last term on the right in both Eqs. (2.4) and (2.13) is related to the thermal emission of holes to the valence band as the temperature increases. At low temperature, this term is insignificant and the remaining term can be solved to give $\tau_0 = (C_{nA}n)^{-1}$ [Eq. (2.3)]. The temperature dependent portion of the lifetime, τ_e,

can be defined as the lifetime of bound holes before they are thermally emitted to the valence band (for $\eta << 1$, as is often the case). From Eq. (2.13), the temperature dependent term gives the lifetime of thermally emitted holes as,

$$\tau_e = (Q_A)^{-1} \tag{2.14}$$

The inverse of the measured PL lifetime can be described as the sum of the inverses of the two lifetimes, τ_0 and τ_e, which can be seen from Eq. (2.13):

$$\frac{1}{\tau} = \frac{1}{\tau_0} + \frac{1}{\tau_e}. \tag{2.15}$$

2.3 External and Internal Transitions

It is helpful to define two types of electronic transitions: external and internal. These transitions are shown as a diagram in FIG. 2.9.

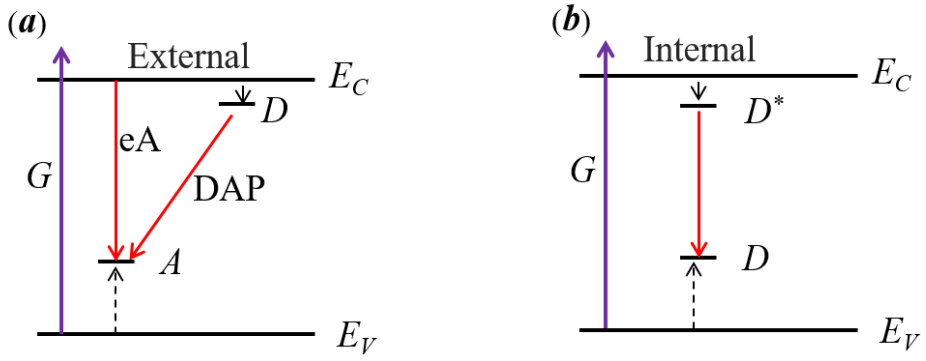

FIG. 2.9: Diagram of (*a*) external PL transitions, and (*b*) internal transitions.

An external transition is what is usually considered to be an electron-hole recombination. An electron from the conduction band or a donor recombines with a hole at an acceptor or in the valence band. For internal transitions, the recombination occurs solely within the defect. An example is an electron localized at a shallow level of the defect which recombines with a hole localized at a deeper level of the same defect. An internal transition can be detected by TRPL,

since for these transitions the PL intensity decays exponentially at any temperature and the PL lifetime is independent of the concentration of free electrons. Defect-related PL originating from internal transitions has been observed in our measurements almost as commonly as those coming from external transitions.

The decay of the PL intensity at various temperatures for external and internal transitions is shown in FIG. 2.10. For T < 50 K, external PL transitions are attributed to DAP recombination which will decay with non-exponential behavior. As the temperature increases above 50 K, the transitions will convert to eA transitions and the PL decay will become exponential. Conversely, for internal transitions, the decay is exponential at any temperature, and independent of the concentration of free electrons.

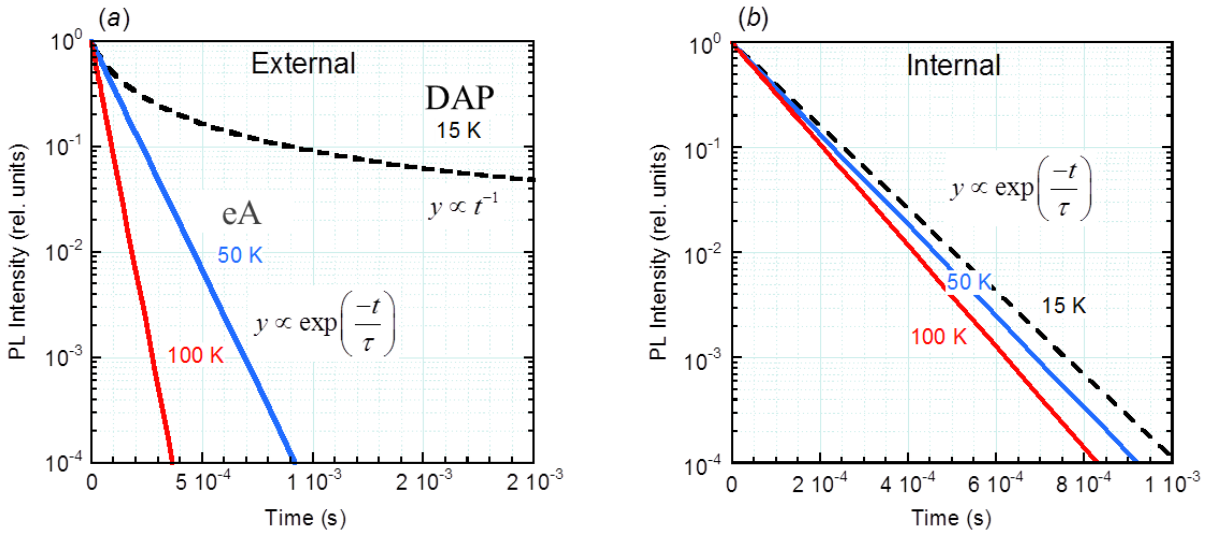

FIG. 2.10: Simulated decay of PL as a function of time for T = 15, 50 and 100 K. (*a*) For external transitions, the PL decay is non-exponential due to DAP recombination, but becomes exponential as DAP transitions convert to eA transitions. (*b*) The PL decay for internal transitions is exponential at any temperature.

2.4 Lifetimes in conditions of PL

In the previous section, the *measured-by-experiment* PL lifetime was discussed, and expressions were found to model the experimental data. It is interesting to note that the *measured*

PL lifetime may be affected by several processes. For example, the lifetime of a hole to escape the valence band depends on capture characteristics of all of the recombination channels, but the time that a particular defect is waiting to capture a carrier is only dependent on the concentration of those free carriers and the defect capture coefficient. In this section, we identify at least 4 different lifetimes for recombination.

Let us consider the lifetime of carrier capture through various channels in an n-type GaN sample, under steady-state conditions of low intensity, above-bandgap light. The generation rate of electron-hole pairs is labeled G, and is determined by multiplying the laser excitation intensity, P_{exc}, by the absorption coefficient, α (10^5 cm^{-1} for GaN), and dividing by the energy of the incident photons, $\hbar\omega_{exc}$:[20]

$$G = \frac{\alpha}{\hbar\omega_{exc}} P_{exc} \tag{2.16}$$

For $P_{exc} = 6 \times 10^{-4}$ W/cm^2, which is below the limit of saturation for these experiments, $G = 10^{20}$ cm^{-3} s^{-1}. The concentration of photo-generated holes is given as p. After the light is turned off, p quickly decays to zero. The concentration of photo-generated electrons (Δn) is insignificant compared to the dark concentration of free electrons ($n \approx n_0$). For a simple case, consider two channels for recombination: a defect center, i with concentration N_i, electron and hole capture coefficients C_{ni} and C_{pi}, respectively, and band to band recombination with a capture rate written as B. To obtain an estimate for the following lifetimes, we can use the following parameters: G = 10^{20} cm^{-3} s^{-1}, $n = 10^{17}$ cm^{-3}, $N_i = 10^{16}$ cm^{-3}, $C_{ni} = 10^{-12}$ cm^{3}s^{-1}, $C_{pi} = 10^{-6}$ cm^{3}s^{-1}, $B = 10^{-11}$ cm^3 s^{-1}. We determine the lifetime of capture for the following cases:

A. A free hole to escape from the valence band
B. A hole to be captured by an *i*-center
C. An electron to be captured by an *i*-center
D. Band-to-band recombination

In each case, the lifetime in question will be the waiting time before a transition of a charge carrier from one place to another, and it will be limited or dependent upon some concentration of either charge carriers or defects. For consistency, each lifetime (*except for the lifetime of holes to escape the valence band*) will be labeled with two subscripts representing 1) the waiting object, and 2) the limiting variable upon whose concentration the transition is dependent.

A. Lifetime for a free hole to escape from the valence band

For low excitation intensities, the lifetime of free holes in the valence band, τ_p, is simply the characteristic time of change in the concentration of free holes after UV illumination has been turned off. It can be found from the equation for the change in the concentration of holes in time:

$$\frac{dp}{dt} = G - Bnp - C_{ni}N_i p \tag{2.17}$$

where $G = 0$ after a laser pulse and the solution is,

$$p = p_0 \exp\left(\frac{-t}{\tau_p}\right). \tag{2.18}$$

For only two channels of recombination, the *i*-center and band-to-band recombination, we can solve for the lifetime of holes in the valence band using Eq.(2.18), and get

$$\tau_p = \left(N_i C_{pi} + Bn\right)^{-1}. \tag{2.19}$$

Eq.(2.19) can be split into the lifetimes for each of the two channels listed. The lifetime of free holes in the valence band depends on the capture rate by the i-center, which is defined as,

$$\tau_{pi} = \left(N_i C_{pi}\right)^{-1}, \tag{2.20}$$

where N_i is the concentration of available centers for the ith channel, and C_{pi} is the hole capture coefficient for that specific center. The lifetime for band-to-band recombination is defined as,

$$\tau_{pB} = (Bn)^{-1}. \tag{2.21}$$

Using the parameters defined above, $\tau_p = 10^{-10} s$. Granted, this is the lifetime of free holes in the limit of low temperatures.

By using a more general form of Eq.(2.17) where more than two channels are competing for the holes in the valence band, we provide a solution for multiple n channels:

$$p = p_0 \left\{ \exp\left[-t \left(\frac{1}{\tau_1} + \frac{1}{\tau_2} + \frac{1}{\tau_3} + ... + \frac{1}{\tau_n} \right) \right] \right\}. \tag{2.22}$$

From this expression, we get the relationship,

$$\tau_p^{-1} = \sum_{i=1}^{n} \tau_i^{-1} = \frac{1}{\tau_1} + \frac{1}{\tau_2} + \frac{1}{\tau_3} + ... + \frac{1}{\tau_n} = \sum_{i=1}^{n} N_i C_{pi} \ , \tag{2.23}$$

where N_i represents any type of defect including band-to-recombination with $N_i = n$ and $C_{pi} = B$.

B. Lifetime of a hole to be captured by an *i*-center

In this section, we will solve for the characteristic time of hole capture by a defect. This may be difficult to measure through experiments, but a theoretical consideration can provide relevant values. We can define two waiting times for this case: the hole waiting in the valence band to be captured by any defect of type i – τ_{pi}; and an individual i-center waiting to capture a hole – τ_{ip}. Here, the i-center will be an acceptor. In the first case, the lifetime is dependent on the concentration of negatively charged i-centers and the hole capture coefficient, C_{pi}, and is not dependent on the concentration of free holes. The rate of capture of holes by the i-center in steady-state PL conditions can be presented as,

$$C_{pi} N_i^- p = \frac{N_i^-}{\tau_{ip}} = \frac{p}{\tau_{pi}}, \tag{2.24}$$

where,

$$\tau_{pi} = [C_{pi} N_i^-]^{-1}, \tag{2.25}$$

and,

$$\tau_{ip} = [C_{pi} p]^{-1}. \tag{2.26}$$

In the first case and for low excitation intensities, $N_i^- \approx N_i$. Then, Eq.(2.25) can be solved to give $\tau_{pi} = 10^{-10} s$.

In the second case, a select *i*-center is waiting to capture a free hole. In contrast to the first case, hole capture by the *i*-center is dependent on the concentration of photo-generated free holes and does not depend on the concentration of *i*-centers. To calculate this lifetime, we have to first solve for *p*. In steady state conditions,

$$G = C_{pi} N_i p + Bnp. \tag{2.27}$$

Solving for *p* gives,

$$p = \frac{G}{C_{pi} N_i + Bn} = G\tau_p. \tag{2.28}$$

Given G = 10^{20} $cm^{-3}s^{-1}$ and τ_p = 10^{-10} s from Eq. (2.19), we find that *p* = 10^{10} cm^{-3}, and thus from Eq.(2.26), $\tau_{ip} = 10^{-4} s$. The lifetime, τ_{ip}, is inversely proportional to the generation rate of electron hole pairs.

C. Lifetime of an electron to be captured by an *i*-center

In a similar fashion, we define two waiting times: the electron waiting in the conduction band to be captured by an *i*-center, τ_{ni}, and a select *i*-center waiting to capture an electron, τ_{in}. In the first case, the lifetime is dependent on the concentration of *i*-centers and the electron capture

coefficient of the defect, C_{ni}. The rate of capture of electrons by the *i*-center in steady-state PL conditions can be presented as,

$$C_{ni}N_i^0 n = \frac{N_i^0}{\tau_{in}} = \frac{n}{\tau_{ni}}, \tag{2.29}$$

where

$$\tau_{ni} = [C_{ni}N_i^0]^{-1}, \tag{2.30}$$

and,

$$\tau_{in} = [C_{ni}n]^{-1}. \tag{2.31}$$

From the rate equation for bound holes at neutral *i*-centers, N_i^0, we have the following expression after a laser pulse:[11]

$$\frac{dN_i^0}{dt} = C_{pi}N_i^- p - C_{ni}N_i^0 n. \tag{2.32}$$

After the laser pulse, *p* goes very quickly to zero as holes disappear from the valence band. The first term on the right-hand-side in Eq.(2.32) can be ignored after approximately $t = 10^{-9}$ s. If the PL recombinations of free electrons with bound holes are much slower, then the solution to Eq.(2.32) with the first term on the right neglected will be,

$$N_i^0 = N_i^0(0)\exp^{\frac{-t}{\tau_{in}}}. \tag{2.33}$$

The PL intensity is $C_{ni}N_i^0 n$, and for *n*-type GaN, *n* is constant. Then the lifetime of the PL due to transitions from the conduction band to the acceptor has the same lifetime, τ_{in}, which is dependent on the concentration of free electrons and the electron capture coefficient. Using the above parameters for an undoped n-type GaN sample, we get $\tau_{in} = 10^{-5} s$.

To find the value for Eq.(2.30), an expression for N_i^0 must be derived. Setting the rates of electron capture and hole capture by an acceptor equal to each other gives,

$$C_{ni} N_i^0 n = C_{pi} N_i^- p \,. \tag{2.34}$$

Given the conditions, it can assumed that $N_i^- \sim N_i$, and an expression for N_i^0 can be given as,

$$N_i^0 = \frac{C_{pi} N_i p}{C_{ni} n} = 10^{15}\ \mathrm{cm}^{-3} \,. \tag{2.35}$$

Thus, from Eq.(2.30), $\tau_{ni} = 10^{-3}\,\mathrm{s}$.

D. Lifetime of band-to-band recombination

This is the waiting time for a free hole to recombine with a free electron. It is distinct from exciton recombination, since that would also depend on the time of capture for the electron to be bound to the hole by the exciton binding energy. The concentration of free holes will be the limiting variable in *n*-type GaN, so we will use the expression for the change in the concentration of free holes after a laser pulse (where $G = 0$), Eq. (2.17). For two channels of recombination, we defined in Eq. (2.19) the lifetime of holes, τ_p, in the valence band as,

$$\frac{1}{\tau_p} = \frac{1}{\tau_{pi}} + \frac{1}{\tau_{pB}} \,. \tag{2.36}$$

This gives us two lifetimes, τ_{pi} and τ_{pB}, the first of which was already shown to be $\tau_{pi} = 10^{-10}\,s$.

and the second expression is represented by Eq. (2.21). Using the value, $B = 10^{-11}$, $\tau_{pB} = 10^{-6}$ s.

2.5 Temperature dependent TRPL

In Ref. 11, the temperature dependence of the PL lifetime decreases almost identically to the decrease in PL intensity in the region of thermal quenching. The explanation for this behavior involves the thermal emission of holes from the acceptor. As the concentration of neutral acceptors decreases with increasing temperature, only electronic transitions from the conduction band which occur with short lifetimes will be possible and transitions with longer lifetimes will

become increasingly less probable. The slope of the decrease in PL lifetime as a function of inverse temperature is identical to the slope of the thermal quenching of the quantum efficiency of PL. In Ref. 11, the lifetime of holes in the valence band is calculated to remain constant for a wide range of temperatures. At some high temperature, the lifetime of thermal emission of holes from the acceptors becomes equal to the lifetime of holes being captured by the acceptors; in other words, τ_p equals Q^{-1}.

Chapter 3: Review of the Literature

The use of time-resolved photoluminescence in the literature primarily consists of analyzing the decay of PL as a function of time at specific wavelengths or energies, in order to measure the characteristic lifetime. A few works report on the evolution of the PL spectra with changing time delay, and a few others on the dependence of excitation intensity and temperature. Most reports in fact deal with the decay of the exciton emission, which is beyond the scope of this particular work and will be excluded. No literature has been found on analyzing the various lifetimes associated with recombination channels, such as the lifetime of holes in the valence band as opposed to the lifetime of PL recombination at an acceptor. The most relevant works to our TRPL studies are presented in this chapter.

3.1 Time-resolved PL spectra

Many works present the PL intensity as a function of energy/ wavelength at a particular time delay or as a function of time. [21,22,23,24] The combination of these two approaches is essentially a 3-dimensional plot which is shown in FIG. 3.1. [25] The emission which results from recombination at defect centers varies in respect to lifetime since the lifetime is a function of the particular defect. If the PL spectra are measured at different time delays, different PL bands may arise due to the different PL lifetimes. The decay of the PL intensity can be both exponential and

non-exponential depending on the nature of the transition, and for exponential behavior, can be modeled by a single exponential expression:

$$I^{PL}(t) = I_0 \exp\left(\frac{-t}{\tau_{PL}(T)}\right). \tag{3.1}$$

As was defined before, $I^{PL}(t)$ is the PL intensity at any moment in time, t, I_0 is the intensity immediately after a laser pulse, and $\tau_{PL}(T)$ is the temperature dependent lifetime of PL. The PL lifetime for band-to-band transitions is given by the relationship, [25]

$$\frac{1}{\tau_{PL}(T)} = \frac{1}{\tau_{rad}(T)} + \frac{1}{\tau_{NR}(T)} + \frac{1}{\tau_{relax}(T)}, \tag{3.2}$$

where the inverse of $\tau_{PL}(T)$ is expressed as the sum of the inverses of the radiative lifetime (rad), the non-radiative (NR) lifetime, and the lifetime of relaxation to lower-lying energy levels. Relaxation occurs as the defect releases excess energy in the form of phonons until it is in the lowest energy level of the excited state. This is typically neglected if radiative transitions occur between the lowest energy states. Note that this expression should be representative of the capture of minority carriers (holes in *n*-type), and is the same expression as Eq.(2.23). It is valid only when τ_{PL} represents the lifetime of band-to-band transitions. It is thus not applicable to the measured PL lifetime related to defects.

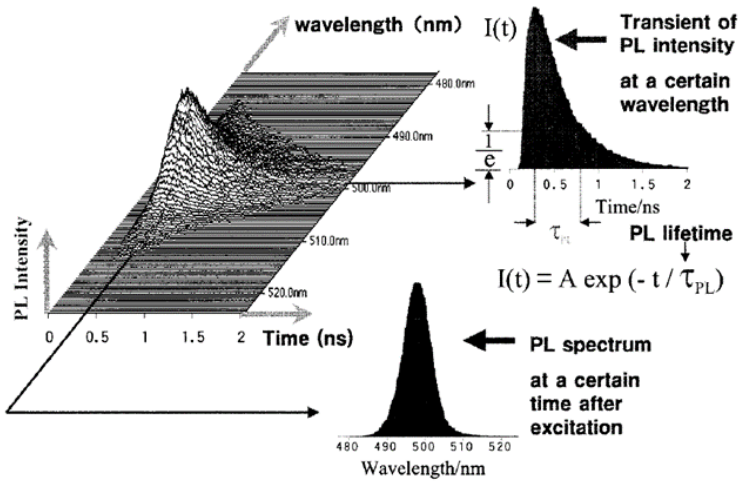

FIG. 3.1: Typical data obtained from TRPL spectra in 3-dimensions of time, PL intensity and PL emission wavelength/ energy. Figure from Ref. 25. Copyright © 1999-2016 John Wiley & Sons, Inc. All Rights Reserved.

3.2 Time-resolved studies on DAP emission

DAP transitions exhibit non-exponential decay behavior, due to the fact that recombinations between the pairs are based on tunneling and coulomb interactions, and not statistical processes. The decay of the PL intensity transforms into exponential behavior as the temperature is increased, as free electrons from the conduction band recombine with holes bound to acceptors (*eA* transitions). This behavior is characteristic of any DAP recombination so that TRPL can identify between DAP related PL bands and those which originate from other sources, such as internal transitions. The PL spectrum measured at various time-delays after the laser pulse can help to distinguish overlapping PL bands in the spectra, and the shift in the PL bands with time often reveals information about the nature of the PL transitions. The PL decay of DAP emission is non-exponential at low temperatures, since the probability of recombination depends on the spatial separation of the donors and acceptors. The rate of recombination between an electron bound to a donor and a hole bound to an acceptor, separated by distance *R*, is given by the expression,[5,29]

$$W(R) = \mathrm{W}_{\max} \exp\left(-\frac{2R}{a_D}\right), \tag{3.3}$$

where W_{max} is the probability for a transition to occur in the limit of least separation; *i.e.*, when $R \to 0$. The Bohr radius of an electron bound to a shallow donor is given by a_D. From this expression, the lifetime of recombination for DAP emission is the inverse of the transition probability: $\tau = W^{-1}$.[5] The non-exponential decay of PL intensity at low temperatures can be described by the expression:[29]

$$I(t) \propto N \exp\left\{4\pi N \int_0^\infty \left[e^{-W(R)t} - 1\right] R^2 dR\right\} \times \int_0^\infty W(R)\, \mathrm{e}^{-W(\mathrm{R})\mathrm{t}}\, R^2 dR, \tag{3.4}$$

where N is the concentration of majority defects (whether donors or acceptors).

An aspect of the non-exponential DAP nature is that the recombinations occur between pairs which have varying spatial separations. Close pairs recombine with fast time-delays, and distant pairs recombine at longer time-delays. Thus the DAP band will red-shift with increasing time-delay, since distant pairs contribute more at longer time-delays and the corresponding energy of emission is less than that of close pairs which contribute at fast time-delays. For deep donors, the shift is expected to be greater than for shallow donors.

As temperature increases, DAP emission gradually transforms into eA transitions, and the energy of emission increases by approximately the ionization energy of the shallow donor. The PL decay becomes exponential when this occurs. Once the PL decay becomes exponential, the lifetime can be described by the inverse of the product of the electron capture coefficient and the concentration of free electrons, as stated previously, or as the maximum of the function $I^{PL}(t) \times t$.[37]

In an earlier work, [26] low temperature PL is studied for DAP transitions in single crystal GaN grown by HVPE. A PL band is observed in the energy range of 3.26 – 2.99 eV, with a ZPL at 3.2571 eV and LO phonon replicas at 3.1672 and 3.0768 eV. The energy difference in the ZPL and the phonon replicas is in multiples of the characteristic LO phonon energy for GaN of 90 meV. The radiative lifetimes of these three peaks are identical, and are much longer than the excitonic lifetimes. This indicates that this band is defect-related and caused by DAP recombinations. With increasing temperature, the ZPL shifts to higher energies consistent with DAP behavior where the electronic transitions change from DAP to recombinations of free-electrons with bound-holes at acceptors (*eA* transitions).

The donor and related acceptor may be spatially separated by varying distances throughout the sample, and the probability of recombination is thus inversely dependent on the distance between them. Close pairs are donors and acceptors which are spatially close with overlapping wave-functions, and have thermodynamic transition levels close to the conduction and valence bands. Distant pairs are spatially distant, with levels further from the conduction band minimum and the valence band maximum.

A schematic drawing of DAP transitions is shown in FIG. 3.2 to show the relationship between close and distant pairs. For DAP transitions, the PL energy at any given photon energy *E* is attributed to the recombination of electrons-from-donors to holes-at-acceptors separated by a specific distance, *r*, and is given by the equation,

$$E = E_g - (E_A + E_D) + E_{Coul.}, \tag{3.5}$$

with,

$$E_{Coul.} = \frac{e^2}{\varepsilon\varepsilon_0 r}. \tag{3.6}$$

Here, the parameters E_g, E_A, E_D and $E_{Coul.}$ are the bandgap, acceptor and donor ionization, and Coulomb energies, respectively, where, e is the electron charge, ε is the dielectric constant for GaN, ε_0 is the vacuum permittivity, and r is the distance between pairs. From the TRPL spectra of the work in Ref. 26, the distance between pairs contributing to PL at 100 μs delay can be calculated to be 120 Å apart, if they use E_g = 3.500 ± 0.010 eV, E_{Coul} = 13 ± 4 meV, E_D = 42 ± 1 meV, E_A = 213 ± 12 meV, and ε = 9.8 for GaN.

The low energy portion of the DAP band consists of contributions from distant pairs, and the high energy portion is due to recombinations between close pairs. With increasing excitation intensity, the distant pairs will saturate leaving the spectrum to be dominated by the recombinations between close pairs, and consequently causing the DAP luminescence peak to blue-shift. In TRPL measurements, close pairs have shorter decay times and distant pairs have longer decay times. The intensity decay from DAP is characteristically non-exponential, which provides a technique for identifying a DAP band within the PL spectrum.

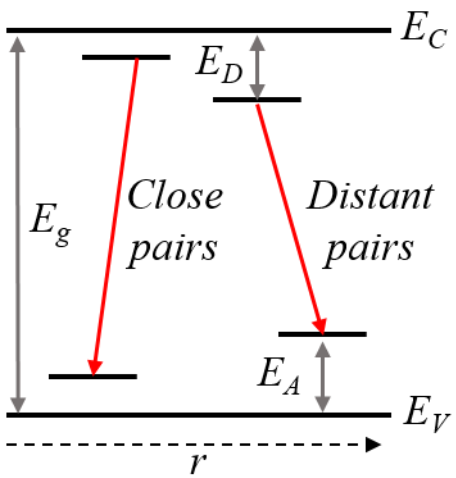

FIG. 3.2: Schematics of DAP recombination. The bandgap, conduction band minimum and valence band maximum energies are labeled E_g, E_C and E_V, respectively. The ionization energies of the donor and acceptor are labeled E_D and E_A, respectively, and the spatial distance between pairs is denoted by r. Red arrows indicate radiative recombination.

TRPL measurements were performed on GaN:Cd and GaN:Zn layers, [27] and the very intense BL was analyzed in both samples. The BL is thought to be caused by transitions through the Zn and Cd related acceptors. In Zn-doped GaN, the broad and very intense BL at 2.89 eV dominates the PL spectrum, but ZPL was observed. Zn doping has been shown in several works to produce several broad emission bands in GaN, depending on the growth conditions and the Zn concentration. In this work, the concentration of Zn is assumed to be 10^{18} cm^{-3}.

The BL decays with a very fast initial component, thought to be the response of the system, and then with two other regions of decay: an exponential decay with a lifetime, τ = 300 ns, and a region of non-exponential decay for time decays greater than 1 μs. The decay with the 300 ns lifetime is supposedly the BL decay of free electrons from the conduction band to holes bound at the Zn_{Ga} acceptor. The subsequent slow, non-exponential decay may be caused by a weak contribution of distant DAP which have much longer lifetimes.[27]

With increasing time delay, the PL spectra do not change much, and the peak energies were very similar even at longer time delays. It seems that there are transitions from both the conduction band to the acceptor (eA transitions) and from the shallow donor to the acceptor (DAP transitions), and these should create PL bands with peaks at different energies. However, the broad spectrum may mask the energy differences of the DAP and eA transitions, since the donor level is predicted to be 30 meV below the conduction band. The broad emission is a result of the strong electron phonon coupling for the Zn_{Ga} acceptor. If the energy lines of two recombination processes are close, then it is difficult to distinguish them in TRPL spectra.

In a simple model for eA transitions, the PL decay can be characterized by the change in the bound hole concentration at the acceptor: [27]

$$\frac{dp_A}{dt} = -C_n n p_A, \tag{3.7}$$

where C_n is the electron capture coefficient, n is the concentration of free electrons, and p_A is the concentration of holes bound to acceptors, which we usually label as N_A^0. The solution of this equation is,

$$p_A = p_A(0)\exp(-t/\tau) \tag{3.8}$$

with,

$$\tau = \frac{1}{C_n n}. \tag{3.9}$$

Bergman et al. estimate that $n = 10^{18}$ cm^{-3} from the level of Zn doping which is also on the order of 10^{18} cm^{-3}.[27] Taking this value and the experimentally found $\tau = 300$ ns, we can estimate that $C_n \approx 3 \times 10^{-12}$ cm^3 s^{-1} for the Zn acceptor in GaN. The binding energy of the Zn_{Ga} acceptor is assumed to be 0.34 eV.

The PL decay for the BL in Mg-doped samples is one of the first TRPL reports on the DAP nature of such PL for a wide range of temperatures. [28] The BL was attributed to an *eA* transition with a lifetime of 900 ps. Kwon et al. argue that such an attribution is inconsistent with other reports. To support this argument, they used the model of Thomas et al. on PL decay for DAP transitions. [29] The time for the intensity of the PL to decay to the value of 1/*e* is given by the expression:

$$\tau = \frac{1}{w(0) N \pi a_B^3}, \tag{3.10}$$

with,

$$w(0) = c E_A^{5/2} E_D^{3/2}. \tag{3.11}$$

w(0) is the recombination rate between the donor and acceptor pair as the separation of the pair $r \to 0$; N is the concentration of the particular defect; a_B is the Bohr radius of the shallower impurity; E_A and E_D are the ionization energies of the acceptor and donor respectively, and c is a constant of the material. By using Eq.(3.10), and the measured value of τ, they postulate values of E_A and E_D from independent calculations to find a value of N which may be comparable to the concentration obtained from SIMS Mg concentrations. In this way, they argue that the BL band in Mg-doped GaN is a result of a transition from a deep donor (possibly V_NMg) to a shallow Mg acceptor.[28]

The behavior of the 2.8 (BL) and 3.2 eV (UVL) bands was studied for Mg-doped GaN.[30,31] Time-resolved measurements show that the lifetime of the 2.8 eV band is 10^{-5} s and that the decay of the PL is non-exponential at low temperature.[32] This points to the fact that the emission is caused by DAP transitions. The positions of the peaks as a function of temperature and excitation intensity were analyzed. The 3.2 band is attributed to transitions from a shallow donor to the shallow Mg_{Ga} acceptor (E_A = 0.2 eV), and the 2.8 eV band is attributed to transitions from a deep donor ($E_D \approx 0.4 – 0.5$ eV) to the same Mg_{Ga} acceptor. With increasing excitation intensity, both peaks of the UVL and BL bands in heavily compensated GaN: Mg shift to higher photon energies. The BL bands shifts substantially by approximately 0.22 eV with increasing excitation intensity by about 7 orders of magnitude.[31] This shift is attributed to the saturation of distant pairs with photo-generated holes at low excitation intensities, such that close pairs dominate the spectrum at high excitation intensity with higher emission energies. The UVL band also blue-shifts by about 0.11 eV with an increase of the excitation intensity of 1000 times, for a *p*-type Mg-doped sample.[31] A different explanation is necessary to explain the shift of the UVL band with increasing excitation intensity. Since the ionization energy of the shallow donor is

approximately 20 meV, the corresponding shift due to close and distant pairs may only be up to half of E_D.[33] The very large shift of ~ 0.1 eV suggests that long-range potential fluctuations exist within the sample. This is very likely for samples which are heavily compensated, as is the case for this work. In samples with an inhomogeneous distribution of charged defects, the potential bands will experience hills near high concentrations of positive charge, and valleys in the presence of high concentrations of negative charges. Transitions between these hills and valleys will be diagonal and the emission energy will be reduced. With increasing excitation intensity, the potential fluctuations will be flattened, and transitions will become vertical with higher emission energy. The shift of the UVL band with increasing excitation intensity may be explained by this phenomenon. It may be interesting to note that in weakly compensated GaN:Mg, the peak shift of the UVL with increasing time-delay is not observed. [30]

The behavior of the UVL and BL bands as a function of temperature was also studied. With increasing temperature, the peak of the BL band shifted by 20 – 40 meV for highest excitation intensities as the temperature increased from 14 to 100 K. At low excitation intensity, the peak position remained almost constant. [31] If a deep-donor is contributing to the BL emission, the strong Coulomb interaction causes the donor level to be more susceptible to thermal ionization, where the close pairs will be ionized first, and then the distant pairs. This may explain the red-shift of the BL peak with increasing temperature, as well as the excitation intensity dependence. The UVL band peak shifted by almost 0.1 eV at lower excitation intensities. This is presumably due to the presence of long-range potential fluctuations. With increasing temperature, carriers are thermally released from the shallower short-range wells and re-captured by deeper ones. Transitions between deeper potential fluctuations have a lower emission energy,

and cause the UVL band to red-shift. Both the BL and UVL bands red-shift with increasing time-delay which is consistent with the deep donor model.[32, 34]

From TRPL measurements on the YL band in Si-doped GaN, [28] Kwon et al, suggest that a shallow Si donor impurity is related to the YL. The PL lifetime at 10K for the YL band decreases from ~650 ns to ~50 ns as the concentration of Si in Si-doped samples increases from $2x10^{18}$ to $1.3x10^{19}$ cm^{-3}. With increasing Si concentration, the PL peaks are red-shifted and broadened, especially on the low energy side. The authors explain this by suggesting that potential fluctuations increase as the concentration of Si increases. However, this may also be caused by strain effects which could also cause a shift in the PL peaks. With Si concentrations of 2.0, 7.2, and 13×10^{18} cm^{-3}, the value of τ decreases and is 650, 110 and 50 ns, respectively. However, the data in Ref. 28 do not follow Eq. (3.10) which may be due to the presence of potential fluctuations. Both the YL and BL in this work exhibit non-exponential PL decay which suggests that they are related to DAP transitions.

The PL lifetime of the YL band varies substantially in the literature. The value of the YL lifetime is given as 20 ps,[35] 1 ns,[36] 50-700 μs,[37,38] or even 300 ms.[39] The decay of the YL is often reported to be non-exponential at low temperatures, and nearly exponential at room temperature. This is a signature of DAP recombination. However, with increasing time delay, the YL does not shift noticeably,[40] as would be expected for DAP transitions involving a deep donor. In fact, the deeper the donor, the larger the red-shift with time-delay. Thus, the lack of red-shift with increasing time-delay signifies that the YL is due to transitions from a shallow donor to a deep acceptor. In other works, red-shifts of 30 – 40 meV and even 100 meV with time-delay are observed for the YL band; however, it must be noted that the appearance of more than 1 type of

YL band have been documented, and thus it is not surprising that the nature of the YL across different samples is complex.

In freestanding GaN, green luminescence (GL) is seen at short time delays less than 10 μs, and afterwards transforms into the YL band with much longer time-delays.[41] The transformation of the GL into the YL decay with increasing time-delay is consistent with the assignment of the two bands to two different charge states of the same defect.[42] In the same samples, the RL and BL bands show persistent PL, and these behaviors are easily explained by the large distances between donor and acceptor pairs, and the relatively low concentration of free electrons.

One of the strengths of the TRPL method is that various PL bands may appear originating from different defects for different time delays, since each transition has a characteristic time delay. It is useful to perform TRPL measurements in order to verify the unique properties and behaviors of each band. In samples of Si-doped GaN, the SSPL and TRPL was measured for 4 samples with increasing Si concentration. [43] Initially, it may seem that the intensity of the defect-related PL increases with increasing excitation intensity in the TRPL spectra for time delays longer than 80 μs. However, upon closer observation, it can be seen that the peak of the defect related band at 2.2 eV varies between 2.2 and 2.6 eV with varying concentrations of Si. It can be argued that the PL is indeed caused by different sources due to the many possibilities of defect formation with increasing dopant concentration. The authors observe a red shift for longer time delays for the 3.27 band with LO phonon replicas. This may be explained by the saturation of close pairs, and the participation of distant pairs at longer time decays. For increasing temperature, a blue-shift of the peak position is observed, which may be a result of *eA* transitions dominating at higher temperatures. The YL band centered at 2.25 eV is observed for all 4

samples, but with different intensities. Other bands which appear at different intensities in the spectra for different samples, such as the 2.35 eV and 2.6 eV bands, indicate that the quality of the samples varied, and perhaps even decreased significantly with increasing Si concentration. The bands are not well defined, and the changing peak positions show that they are not related to the same transitions.

The red luminescence band in cubic GaN was studied, [44] and from TRPL data was shown to have the same characteristics of the yellow luminescence band in wurtzite GaN. In the TRPL measurements, the peak of the RL band (in cubic GaN) shifts from higher energy to lower energy for increasing time delays, corresponding to the behavior of close pairs contributing at shorter decay times and distant pairs contributing at longer decay times. The decay of the PL intensity is non-exponential which also points to DAP transitions. Since the bandgap of cubic GaN is E_g = 3.3 eV at 4.2 K which varies significantly from the value in wurtzite GaN of E_g = 3.50 eV at 2 K, acceptors in cubic GaN have smaller ionization energies than in wurtzite phase GaN. Goldys et al. suggest that the YL band in wurtzite GaN is related to the same transitions of the RL band in cubic GaN. Specifically, this may be a transition from a shallow donor to a deep acceptor with strong electron phonon coupling. The YL band has a similar line shape to the RL band in cathode luminescence of cubic GaN. This may indicate that they may originate from the same transition. Additionally, the RL band blue-shifts with increasing excitation intensity, which is consistent with DAP behavior.

3.3 TRPL in GaN-related systems and other semiconductors

Incorporating As into GaN is known to produce a series of deep traps that can cause a broad signal to be emitted in the 2.6 eV range.[45] Sometimes labeled BL, the intensity of this

emission depends strongly on the N/Ga flux ratio during plasma assisted MBE growth. It is the most intense in samples grown under N-rich conditions. It has been reported that the bandgap of GaN:As decreases as the composition of As increases.[46] Under N-rich conditions the As atoms may replace Ga atoms and behave as deep donors, and cause the intense emission in the 2.6 eV range. The experimental data for the PL spectrum at 8K show peaks at 2.4 and 2.57 eV. As the temperature is increased to 150 K, the 2.57 eV peak blue-shifts to 2.61 eV, then interestingly shifts back to 2.57 eV, but broader, at 300 K. The PL intensity does not vary much with increasing temperature, which suggests that the traps are too deep for thermal activation. The decay of the 2.6 eV emission can be fit with a single exponential, and shows that the lifetime of the PL first decreases from 90 to 80 ns for the temperature range 8 – 100 K, then increases from 80 to 150 ns for the temperature range 100 – 300 K. Gil et al. suggest that the increase in the time delay with increasing temperature is due to inefficient non-radiative recombination. The attribution for this transition comes from calculations performed by Van de Walle and Neugebauer.[47] They calculate that the formation of the As_{Ga}^{2+} defect is energetically favorable. This double charge deep donor state may be the cause of the intense 2.6 eV emission in GaN:As. Such an attribution may be justified because of the long decay times which are characteristic of large lattice relaxation. This is consistent with theoretical predictions that the As incorporated into the Ga site behaves as a deep donor, negative-U center, where the center can bind two electrons, with the second electron being more tightly bound than the first due to large lattice relaxation of the first charge state.

PL lifetime studies were performed for heavily-doped GaAs:Si, and the emission from the Si_{Ga} defect was studied.[48] A defect in GaAs:Si, called the Si-Y defect in this work, is supposedly the origin of the 1.2 eV band where transitions occur from near the conduction band

through this defect. The lifetime of this emission remained mostly constant for the temperature range of 20 – 200 K with an average value of 10 ns. This seems unusual since the intensity of the PL decreases with increasing temperature above 100 K, and this causes competition between the radiative and non-radiative channels, such that the measured lifetime is expected to decrease. Evidently, the thermal emission of electrons should not have any effect on the behavior of the thermal quenching since the sample is heavily doped and is degenerate.

Interestingly, Saucy et al. suggest that the radiative recombinations are faster than non-radiative recombinations, and thus non-radiative transitions do not affect the measured lifetimes. Also Saucy et al. are unable to explain why the lifetime is constant with temperature. It is an open question what exactly is being measured as the PL lifetime, since the lifetime does not necessarily agree with other works. From Williams et al,[49] the $V_{Ga}Si_{Ga}$ and the $V_{As}Te_{As}$ complexes are very similar, the V_{Ga} dictates the behavior of the defect and not the shallow donor. Although the lifetimes of PL from the $V_{Ga}Si_{Ga}$ complex are not determined, the lifetimes of PL from the $V_{As}Te_{As}$ complex have been reported in great detail, and the range is between 0.1 and 50 μs for many samples with varying concentrations of free electrons.[50]

The electron capture coefficient of the Si-Y defect, which is called by others the $V_{Ga}Si_{Ga}$ complex with an activation energy of 0.18 eV, is unknown. However, using the value of the electron capture coefficient from the $V_{As}Te_{As}$ complex (maximum at 1.2 eV), a very similar defect, the lifetime of PL through this channel may be estimated. From Ref.(50), $C_{ni} = 1.3 \times 10^{-12}$ $cm^3\ s^{-1}$. Saucy et al. state that the concentration of free electrons in these samples is $n = 4.9 \times 10^{18}\ cm^{-3}$. From Eq.(2.31), the expected lifetime for these samples can be estimated to be about 160 ns.

3.4 Lifetimes in giant traps and cascade capture

Giant traps in Ge and Si semiconductors were first studied by Lax [61] who developed a model for the cascade capture of electrons. A giant trap, or an attractive center with a large capture cross-section in the range of 10^{-15} to 10^{-12} cm^2, can bind an electron to an excited state with higher probability than to the ground state. An electron bound to a giant trap will dissipate energy by interacting with phonons and transitioning downwards through a series of Coulomb excited states. Lax proposed that the sticking probability of an electron in the giant trap is proportional to *kT*, and with decreasing temperature, the capture cross-section will begin to increase dramatically. In his model, the electron after emitting a single phonon transitions from the conduction band to a level of the giant trap which is on the order of *kT*. The cross section according to Lax is,

$$\sigma \sim \pi r_T^2 \frac{r_T}{l}\left(\frac{ms^2}{kT}\right)^2 \tag{3.12}$$

where r_T is the radius of the attractive center, *l* is the mean free path of the electron, and *m* and *s* are the effective mass of the electron and the speed of sound, respectively. Lax, however, did not take into account that an electron may be bound to a state with energy less than *kT* with the possibility of being thermally ejected back into the conduction band. Abakumov and Yassievich[10] showed that the capture cross section must take into account this thermal ejection for energies less than *kT* and proposed the following revised formula for the capture cross section:

$$\sigma = \frac{4}{3}\frac{\pi}{l_0}\left(\frac{e^2 Z}{\kappa kT}\right)^3 \tag{3.13}$$

with $l_0 = v\tau_e$ (which does not depend on the electron energy or the temperature), *eZ* is the center charge, and κ is the dielectric constant. In this relationship, the capture cross section decreases by the cube of inverse temperature. Since the lifetime of capture by a center is inversely proportional to the capture cross section, it is expected that the lifetime of capture by a giant trap will increase with increasing temperature.

Chapter 4: Resolving PL bands in undoped and Si-doped GaN

Photoluminescence, the emission of light, occurs in a material after stimulation by light. From an early work of Gurney and Mott, PL caused by resonant excitation of an electron from a defect to the conduction band is described as the following: "The emission energy is less than absorption energy. After light is absorbed, and the electron moves into an excited state, the surrounding ions or atoms are no longer in equilibrium in the new field which exists around the exciton; in a time of 10^{-13} – 10^{-12} s, they will move into their new positions of equilibrium, the excess energy being taken up by the vibrations of surrounding atoms and thus conducted away in the form of heat." [51] Indeed, the study of PL from GaN reveals that there are complex interactions among photons, electrons, phonons, individual ions, and the surrounding ions. Thus, PL studies provide valuable information on an intricate system.

4.1 Defect-related photoluminescence in GaN

The SSPL spectra of many GaN samples have been analyzed, and the spectra of two undoped GaN samples are shown in FIG. 4.1. PL bands are labeled based on the color and energy of emission, such as red, yellow, green, blue and ultraviolet luminescence (RL, YL, GL, BL and UVL). These PL bands originate from various defects, and can be distinguished one from another by analyzing the PL lifetime, PL decay, TRPL spectra, thermal quenching of the

PL intensity, and in some cases, the peak position and ZPL. The following discussion divulges basic information on the properties of several PL bands which were studied for this work.

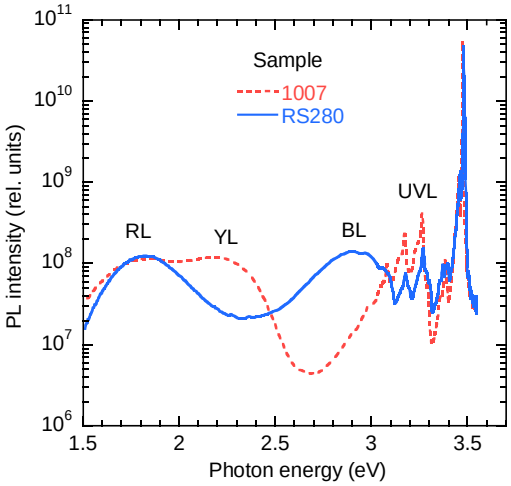

FIG. 4.1: Steady-state PL spectra for undoped GaN samples 1007 and RS280 at T = 18 K, and for excitation intensity P_{exc} = 10^{-3} W/cm^2. RL, YL, BL and UVL defect-related bands are labeled.

A. Red luminescence

In HVPE grown GaN, an RL band is often observed with a maximum at 1.8 eV. There may be several origins of red luminescence and careful measurements must be conducted to determine which band is present in a given sample. In particular, RL1 is characterized by non-exponential PL decay for T = 15 K, and has a very long PL lifetime for temperatures between 100 and 300 K.[5] Its behavior is characteristic of DAP transitions at low temperatures, and is attributed to electron transitions from shallow donors (at T < 40 K) and from the conduction band (for T > 40 K) to a deep defect level. No fine-structure has been observed for this band as of yet. Another RL band is frequently seen in high-resistivity GaN grown in Ga rich conditions, and is called RL2. It is characterized by an internal transition through some unknown defect due to the exponential PL decay at any temperature. The PL lifetime for RL2 is distinct since it decreases from 110 to 2 μs as the temperature increases from 15 to 100 K.[5] A third RL band, labeled RL3, is seen in some HVPE GaN samples where RL1 is not present. The ZPL of the RL3 band has

been observed at 2.36 eV.[52] However, recent TRPL measurements indicate that this particular ZPL should be attributed to another YL band. TRPL measurements of the RL3 band show exponential PL decay (internal transition) and a very fast lifetime of 15 – 20 ns for temperatures 15 to 200 K. Both RL1 and RL3 may be present in HVPE grown GaN, but the reason for one band to be manifested over another is not currently known. However, one can be clearly distinguished from another through TRPL measurements.

B. Yellow luminescence

Another interesting set of PL bands are the YL bands whose origins have been the topic of many discussions.[5] In GaN, there seem to be several different defects which cause YL, and it is sometimes difficult to distinguish the nature of the YL when its intensity is weak or when other PL bands are overlapping. One YL band has been clearly identified due to its characteristic band shape and fine-structure. This band is labeled YL1 and has a maximum at 2.20 eV and a ZPL at 2.57 eV at low temperatures.[53] YL1 is observed in undoped, Si-doped and C-doped GaN, grown by HVPE and MOCVD.

C. Green Luminescence

At times, the PL spectra clearly show certain bands but obscure others. Such is the case for the GL in HVPE grown GaN. In FIG. 4.1, it is possible to identify the RL1, YL1, BL1 and UVL defect related bands, but the GL is hidden in the steady-state spectra. For short time delays (~0.3 μs) in TRPL spectra, the GL band is clearly seen dominating over the rest of the bands. With increasing time delay, the time-resolved spectra evolve into other bands whose lifetimes are longer than the GL. This particular GL band, which is hereafter called GL1, has a maximum at 2.4 eV, and is commonly seen in conductive *n*-type GaN.[5] After the laser pulse, the decay of the GL1 is exponential even for low temperatures, and has a characteristic lifetime of 1 – 2 μs for the

temperature range of 15 to 100 K. The PL lifetime after 100 K for this band increases with increasing temperature, which is contrary to every other PL band in GaN thus far. This behavior is very interesting and leads to important conclusions, but will be addressed in further detail in Chapter 5. The origin of the GL1 can be attributed to an internal transition between an excited state and ground state of a defect, with the excited state behaving as a characteristic giant trap.[10,61,62] Another GL band found in high-resistivity GaN with a peak at 2.36 eV is called the GL2 band, and is the result of an internal transition of the V_N defect.[19]

D. Blue luminescence

In several samples, a blue luminescence band with a peak at 2.9 eV can be well resolved at low temperatures (samples RS280, 1601, T1011, and T2015). This band, labeled BL1, is attributed to Zn_{Ga} acceptors which are unintentionally introduced during the HVPE or MOCVD growth of GaN.[5] In some samples, a strong UVL band obscures the BL1 band for temperatures below 120 K, but as the UVL band is thermally quenched, the BL1 band can be clearly seen for the temperatures between 150 and 200 K (samples 104, 201, 202, 203). The BL1 band is thermally quenched at $T > 180$ K with an activation energy of 0.35 eV. Thermal quenching of the BL1 is caused by thermal emission of holes from the Zn_{Ga} acceptor to the valence band with increasing temperatures. In high resistivity GaN, a different BL band, called BL2, is observed with a maximum at 3.0 eV, and is caused by carbon-hydrogen complexes.[54]

E. Ultraviolet luminescence

Finally, the UVL band with a peak at 3.26 eV is seen in almost all the GaN samples studied in this work, with its strongest contribution at low temperatures. The UVL band begins to thermally quench for $T > 100$ K and completely disappears by $T = 200$ K. Thermal quenching of

the UVL is caused by thermal emission of holes from an unknown shallow acceptor to the valence band with increasing sample temperature.

F. Fitting the shape of PL bands

The shape of PL bands can be fit using an equation previously stated, but included here for convenience [see Eq. (2.8) and FIG. 2.6]:

$$I^{PL}(\hbar\omega) = I^{PL}_{\max} \exp\left[-2S_e\left(\sqrt{\frac{E_0^* - \hbar\omega}{E_0^* - \hbar\omega_{\max}}} - 1\right)^2\right] \tag{4.1}$$

Usually the GL1 band is not clearly resolved in the PL spectrum, until certain experimental conditions are satisfied (high excitation intensity, etc). The GL1 is clearly resolved when it has a relatively high intensity and minimal overlap with other bands. In this case, Eq.(4.1) can be used to fit the shape of the GL1 band, and the specific parameters which provide the shape of the GL1 band can be determined. When the spectra contain overlapping bands, these parameters can be used to fit the shape of the bands and determine the relative contribution of each band to the spectrum. The parameters for the major bands in undoped GaN are listed in Table 4.1.

Table 4.1. Parameters in Eq.(4.1) which describe the shape of PL bands in undoped GaN.

PL band	$\hbar\omega_{\max}$ (eV)	E_0^* (eV)	S_e
RL1	1.78	2.22	6.5
YL1	2.2	2.66	7.4
GL1	2.4	2.92	8.5
BL1	2.9	3.15	2.2

4.2 Excitation Intensity Dependence

Ideal experimental conditions are necessary to reveal certain bands in the PL spectrum. Varying the excitation intensity for SSPL is one means to reveal hidden bands as has been

suggested. In FIG. 4.2, the SSPL spectra for undoped GaN sample RS328 are shown for the RL1, BL1 and UVL bands, which are all present for the range of excitation intensities used. In undoped GaN sample 1007, we observe the YL1 band and not the BL1 band (FIG. 4.3).

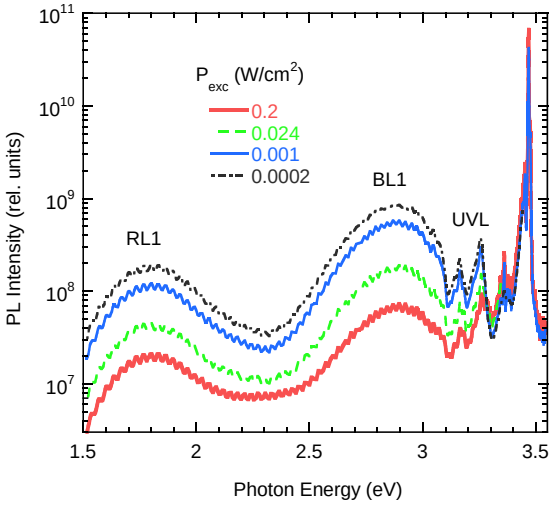

FIG. 4.2: SSPL spectrum at T = 18 K of undoped GaN sample RS328 for P_{exc} = 2.9×10^{-5} – 0.2 W/cm^2. Near-band-edge emission is the peak at highest energies, followed by UVL and its phonon replicas. The BL and RL are broad defect-related bands. The long range oscillations are caused by Fabry-Perot interface in the thin GaN layer.

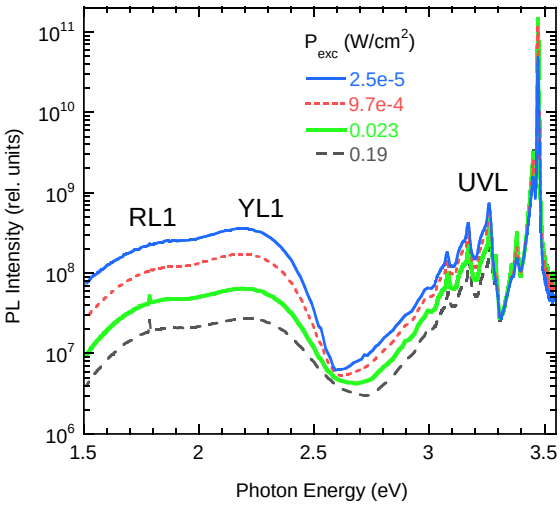

FIG. 4.3: SSPL spectrum at T = 18 K of undoped GaN sample 1007 for P_{exc} = 2.9×10^{-5} – 0.2 W/cm^2. The near-band-edge emission is the first peak at highest energies, followed by UVL and its phonon replicas. YL and RL bands are present at lower photon energies.

However, if the excitation intensity is increased for undoped GaN sample RS280, the GL1 suddenly emerges, as can be seen in FIG. 4.4. In other studies,[55,60] it has been shown that the

GL1 band has a super-linear dependence on excitation intensity, since it originates from a defect which must first capture two holes before emitting GL1.

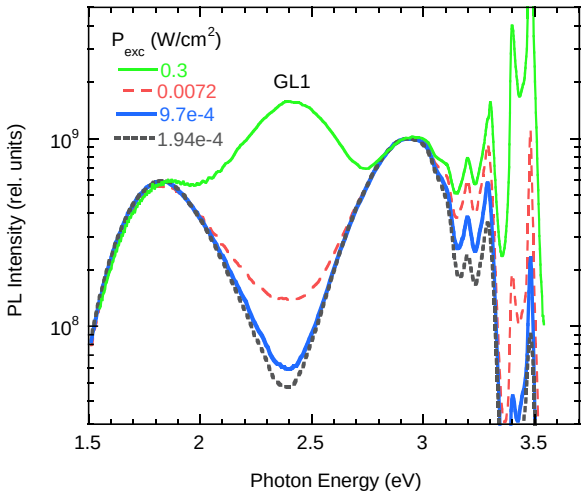

FIG. 4.4: SSPL spectra of undoped GaN sample RS280 at T = 100 K, for P_{exc} = 7.2×10^{-3} – 0.3 W/cm^2. The exciton peak is cut for intensities above 5×10^9 rel. units. UVL, BL and RL bands are present for all excitation intensities, and GL rises super-linearly with increasing P_{exc}.

4.3 Temperature dependence of PL Intensity

Thermal quenching of PL bands occurs when holes bound to the related acceptors are thermally emitted to the valence band with increasing temperature. In this way, the intensity of the PL band will decrease with an activation energy related to the ionization energy of the defect. The thermal quenching of the RL, GL1, BL1 and UVL are shown in FIG. 4.5. All four bands are clearly resolved in this sample for the sample conditions given in the figure caption. However, in other spectra, one band may obscure another band until it is thermally quenched. For example, the UVL band in FIG. 4.6 quenches around 120 K and reveals a hidden BL1 band in undoped GaN sample RS320. Additionally, the RL band quenching reveals a YL1 band as a shoulder for T = 180 K. While the UVL is quenched by 180 K, and the BL1 by 270 K, the YL1 band does not quench until 450 K, as can be seen in other measurements, not shown here.

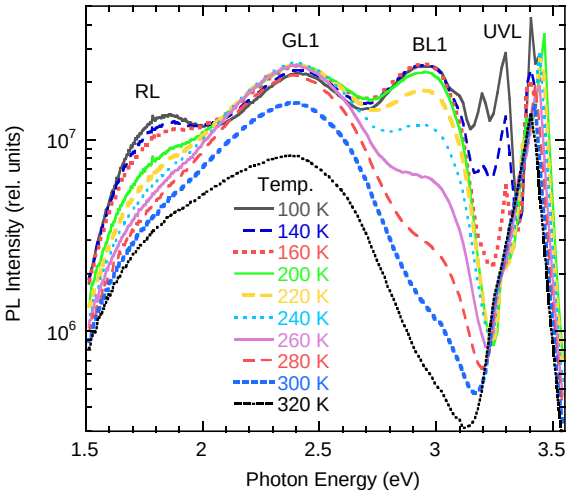

FIG. 4.5: Temperature dependence of the SSPL spectra for undoped GaN sample RS280. Four defect-related bands are present at 100 K: UVL, BL1, GL1 and RL for P_{exc} = 0.19 W/cm^2. By T = 320 K, all bands have significantly quenched except for the GL1.

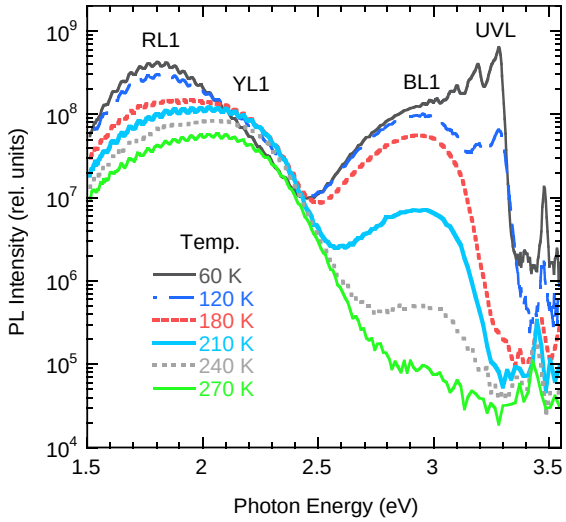

FIG. 4.6: Temperature dependence of the SSPL spectra for undoped GaN sample RS320. P_{exc} = 0.02 mW/cm^2. The UVL band begins to quench around T = 120 K, and reveals the BL band which quenches after T = 180 K. The YL and RL bands are not clearly resolved, but the RL in this case shows thermal quenching beginning around T = 150 K.

4.4 Time-delay dependence of PL bands

In TRPL, the decay of the PL intensity is measured as a function of time at select photon energies. The intensities of the PL for given time delays after the laser pulse are plotted for the

select photon energies and form a spectrum, as is shown in FIG. 4.7 for undoped GaN sample 1007. The bands are fit using Eq. (4.1), and the parameters are listed in the caption.

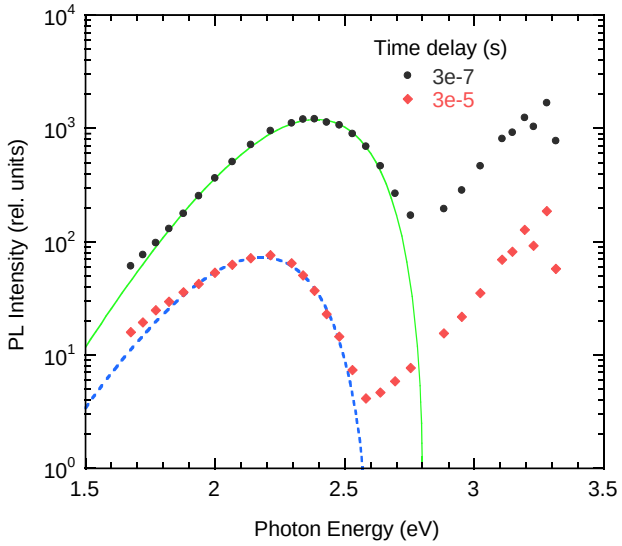

FIG. 4.7: TRPL spectra at 0.3 and 30 μs after the laser pulse, for undoped GaN sample 1007. At fast time delays, a GL band is seen with a peak at ~ 2.4 eV, and at longer time delays, and YL band with a peak around 2.2 eV becomes evident. T = 100 K**.** The bands are fit using Eq. (4.1) and the following parameters: (GL) S_e = 8.5, $\hbar\omega_{\max}$ = 2.40 eV, and E_0^* = 2.92 eV; and (YL) S_e =7.4, $\hbar\omega_{\max}$ = 2.20 eV, and E_0^* = 2.62 eV.

The SSPL data can be compared with TRPL spectra to show that the same bands are being analyzed. In FIG. 4.8, the UVL band is clearly seen at 0.1 μs in the TRPL spectrum and the SSPL agrees. The lifetime of the UVL, τ, is about 20 μs. The GL1 band is present in the TRPL spectrum for short time delays at 0.1 μs, with τ = 2 μs, but is not seen in the SSPL spectrum. With increasing time delay, the YL1 band emerges with a lifetime of 0.5 ms. Finally, the RL1 appears in the TRPL spectrum after 1 ms and has a lifetime $\tau \approx$ 1 ms. These data show very clearly the dependence of a PL band on time delay, and how it is possible to distinguish PL bands based on their characteristic and (usually) unique lifetime. This is very useful especially when PL bands are not easily distinguished. For example, in undoped GaN sample H202 shown in FIG. 4.9, with increasing time-delay, the GL1 band merges into a weakly resolved YL1 band.

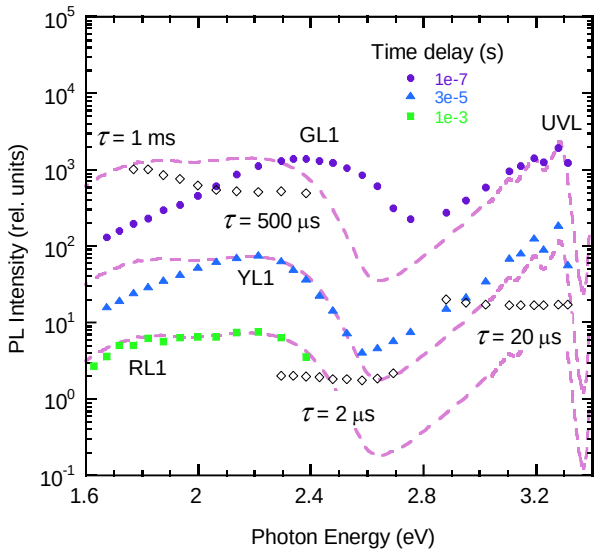

FIG. 4.8: TRPL spectra (filled symbols) for undoped GaN sample 1007, for time delays of 0.1 – 3×10^3 μs. SSPL spectra at T = 100 K taken for P_{exc} = 9.6×10^{-4} W/cm^2 is plotted three times (dashed lines) but arbitrarily shifted to compare the PL bands observed in TRPL and SSPL. Both spectra clearly show the UVL band at any time delay. At short time delays, the TRPL show a GL band which is not seen in SSPL. At longer time delays, the TRPL spectra show RL1 and YL1 bands in agreement with the SSPL. The lifetimes of the UVL, GL1, YL1 and RL1 bands are shown with open diamond symbols.

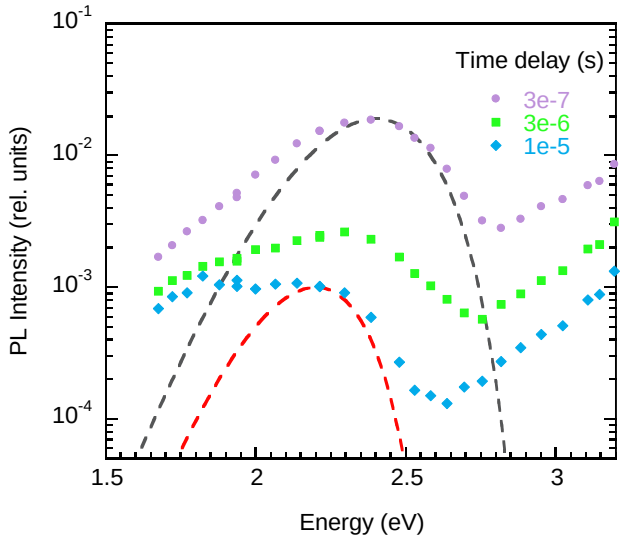

FIG. 4.9: TRPL spectra for time delays of 0.1 – 3×10^3 μs. Sample is undoped GaN H202, T = 100 K. The shape of the GL band seen from 0.3 to 1 μs and the YL band seen at 10 μs can be fit using Eq.(4.1) and the following parameters: (GL) S_e = 8.5, $\hbar\omega_{\max}$ = 2.40 eV, and E_0^* = 2.92 eV; and (YL) S_e =7.4, $\hbar\omega_{\max}$ = 2.20 eV, and E_0^* = 2.62 eV.

Eq. (4.1) can be used to reveal the YL1 band using parameters obtained from more clearly resolved bands.

4.5 A new red luminescence band

Red luminescence is easily identified in TRPL measurements. Previously, data have been shown for the RL1 band which has a characteristic PL lifetime of about 1 ms. Another RL band can also be seen in HVPE grown undoped GaN, except with a characteristic lifetime of about 20 ns. This fast RL3 band, as it is called, can be seen in GaN samples when the RL1 band is not dominating the low-energy portion of the spectrum. In FIG. 4.10, the SSPL spectra are shown for undoped GaN sample RS280, with the RL3 band and the UVL and BL1 bands. The best way to identify the RL3 band is to perform TRPL measurements, since the RL3 band very quickly decays after a laser pulse. In FIG. 4.11, the time delay TRPL spectra are shown for 0.01 – 100 μs. At time delays less than 100 ns the RL3 band is the dominant defect-related band at the low energy side of the spectrum in both the TRPL and the SSPL.

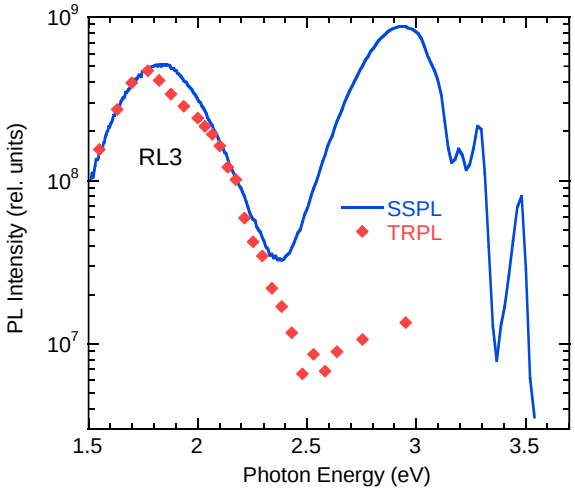

FIG. 4.10: SSPL (P_{exc} = 2.5×10^{-5} W/cm^2) and TRPL (N=0.0008) spectra for undoped GaN sample RS280, for T= 100 K. The time delay for the RL band is less than 20 ns, which indicates it is different from the commonly observed RL1 band with a time delay of ~ 1ms.

For increasing time delay, the RL3 transforms into the YL3 band which should also be distinguished from the well-studied YL1 band. The spectra in FIG. 4.11 are measured through the sapphire substrate which shows that the RL3 related defect is present in the bulk and at the

GaN/ sapphire interface, and is not surface–related. Both the RL1 and RL3 bands contribute to the SSPL spectra in samples where the RL3 is observed. It is difficult to distinguish one from the other in the SSPL spectra, and thus enhances the benefit of performing TRPL measurements to confirm the contribution of each band.

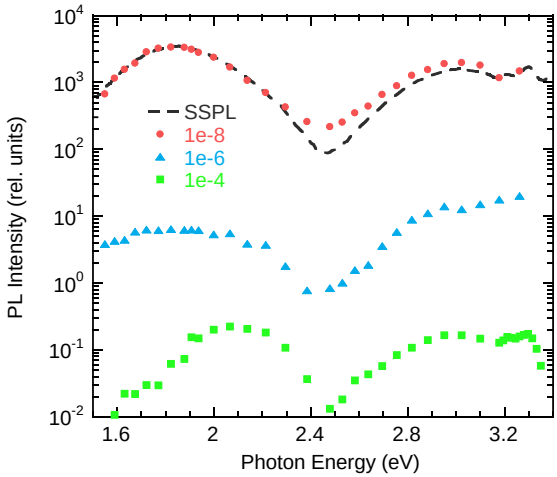

FIG. 4.11: SSPL (P_{exc} = 0.128 mW/cm^2) and TRPL (N=0.01) spectra measured through the sapphire substrate for undoped GaN sample RS280, for T = 100 K. The presence of the fast RL3 band indicates it is not a surface-related effect, but originates from defects in the bulk and at the GaN/sapphire interface. Other defect-related bands are the UVL, BL, and YL at longer time delays.

4.6 Finding the ZPL for yellow luminescence

The yellow luminescence band in GaN is the source of much controversy in the scientific community. It is practically ubiquitous in most room temperature PL spectra of intentionally and unintentionally doped GaN samples. The shape of the YL band is asymmetric and non-Gaussian, most likely due to electron-phonon interactions. The peak of the YL is typically centered-around 2.20-2.25 eV. The center which causes the YL has been discussed for decades, and propositions have included Ga-vacancies, damage from ion implantation, carbon impurities, and various types of complexes involving dopants.[5] The nature of the YL transition is also disputed. Early works attributed the YL band to transitions between shallow donors and deep acceptors, and although other more complex models proposed transitions between deep-double donors and acceptors, the

simpler model has won out. The shape, and temperature dependence of the YL suggests a simple donor-acceptor type transition. The origin of the defect remains unknown, albeit there are several good candidates at the moment. Until recently, the fine structure and ZPL have not been observed for the YL band. As will be shown below, steady-state and time-resolved studies reveal the fine structure of the YL in HVPE grown undoped GaN, and MOCVD grown Si-doped GaN.[53] The fine-structure arises from the superposition of PL lines caused by local and LO lattice phonons. The YL band is shown to be identical in both Si-doped and undoped GaN and coming from the same defect.

HVPE grown undoped GaN exhibits the most clearly resolved ZPL, and the SSPL spectra for sample H202 is shown in FIG. 4.12.

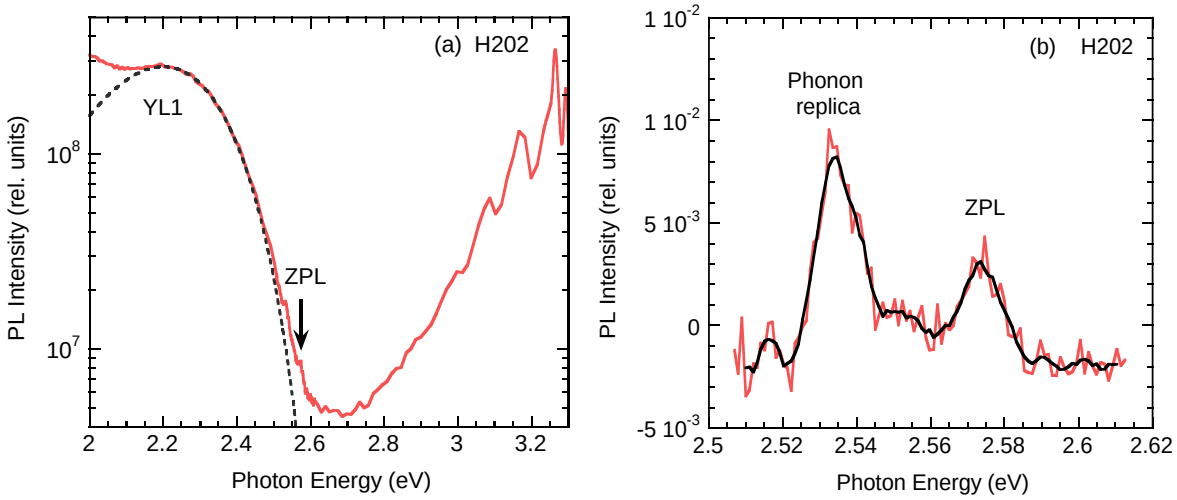

FIG. 4.12: (***a***) SSPL spectra of undoped GaN sample H202, where T = 18 K, and P_{exc} = 0.0002 W/cm^2. The ZPL is seen at the high-energy side of the YL band. (**b**) Fine structure of the YL band in undoped GaN sample H202, obtained after subtracting the smooth component of the YL band using Eq.(4.1). T= 18 K, and P_{exc} = 0.0002 W/cm^2.

The ZPL is indicated on FIG. 4.12 (a) with an arrow, and can be more clearly seen in FIG. 4.12 (b). To reveal the the fine structure of the yellow luminescence, we subtract the smooth component of the YL1 band obtained from Eq. (4.1).

The SSPL and TRPL spectra of Si-doped GaN sample cvd3540 grown by MOCVD are shown in FIG. 4.13. The peak of the YL band in Si-doped GaN is 2.22 eV, which is 0.02 eV higher in energy than in undoped GaN grown by HVPE. The blue-shift is due to the Fermi level being shifted for degenerate, *n*-type GaN:Si. The shallow donors near the conduction band form a band of energies, and the corresponding transitions from this band of donor energies will be higher in energy. Although the ZPL is not as clearly seen in Si-doped GaN samples, it can be attributed to the abrupt drop in PL intensity at the high-energy side of the YL band at about 2.6 eV. The shape of the YL band in Si-doped GaN can be fit with the same parameters as undoped GaN grown by HVPE and MOCVD, and thus we conclude that the YL band in undoped, unintentionally doped and Si-doped GaN is identical and caused by the same defect.

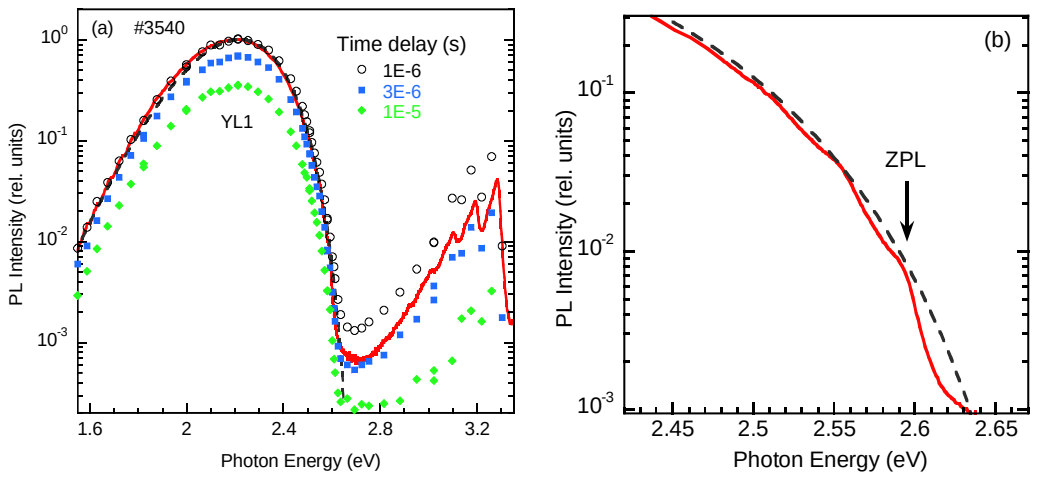

FIG. 4.13: ***(a)*** Normalized PL spectrum of Si-doped GaN sample cvd3540 grown by MOCVD. T = 18 K, and P_{exc} = 1 mW/cm^2. Steady-state spectra is shown by the solid line, and the TRPL spectra is shown by the symbols taken 1-10 μs after the laser pulse. The shape of the band shown by the dashed line is fit with Eq.(4.1) and the following parameters: $I_{\max}^{PL}$ = 1, S_e= 7.4, E_0^* = 2.68 eV, and $\hbar\omega_{\max}$ = 2.22 eV. The data for the TRPL and SSPL are normalized at the maximum for t = 1E-6 s. ***(b)*** A zoomed-in region of the SSPL spectrum near the ZPL.

4.7 Temperature dependence of the PL lifetime

A useful way to determine important information regarding a PL band is to analyze the temperature dependence of the PL lifetime. This can be done using formulas which were shown

in Chapter 2, and will be included here for convenience. The thermal quenching of the quantum efficiency was shown to be,

$$\eta_A(T) = \frac{\eta_0}{1+(1-\eta_0)\tau_0 Q_A}, \tag{4.2}$$

where the parameters were explained in Section 2.1 A. Interestingly, the PL lifetime as a function of temperature behaves in almost the same manner as the quenching of the quantum efficiency, and can be described by the expression,[11]

$$\tau = \frac{\tau_0}{1+(1-\eta_0)\tau_0 Q_A} \tag{4.3}$$

Again we state that,

$$Q_A = C_{pA} N_v g^{-1} \exp\left(-\frac{E_A}{kT}\right), \tag{4.4}$$

and,

$$\tau_0 = \frac{1}{C_{nA} n} \ . \tag{4.5}$$

According to Eq.(4.2), the PL intensity (which is proportional to the quantum efficiency) is temperature independent for temperatures below thermal quenching, but decreases exponentially for $T > T_0$ where T_0 is the characteristic temperature found when $(1-\eta_0)\tau_0 Q_A = 1$ in Eq.(4.2). Similarly, the PL lifetime changes with temperature with the exception that at low temperature, the lifetime is not constant (as is expected for the PL intensity) but decreases for non-degenerate samples since n is temperature dependent. The temperature dependence of the PL lifetime for undoped GaN samples H202, H203, RS331, RS330 and RS328, for the RL1, YL1, GL1, BL1, and UVL bands is shown in FIG. 4.14.

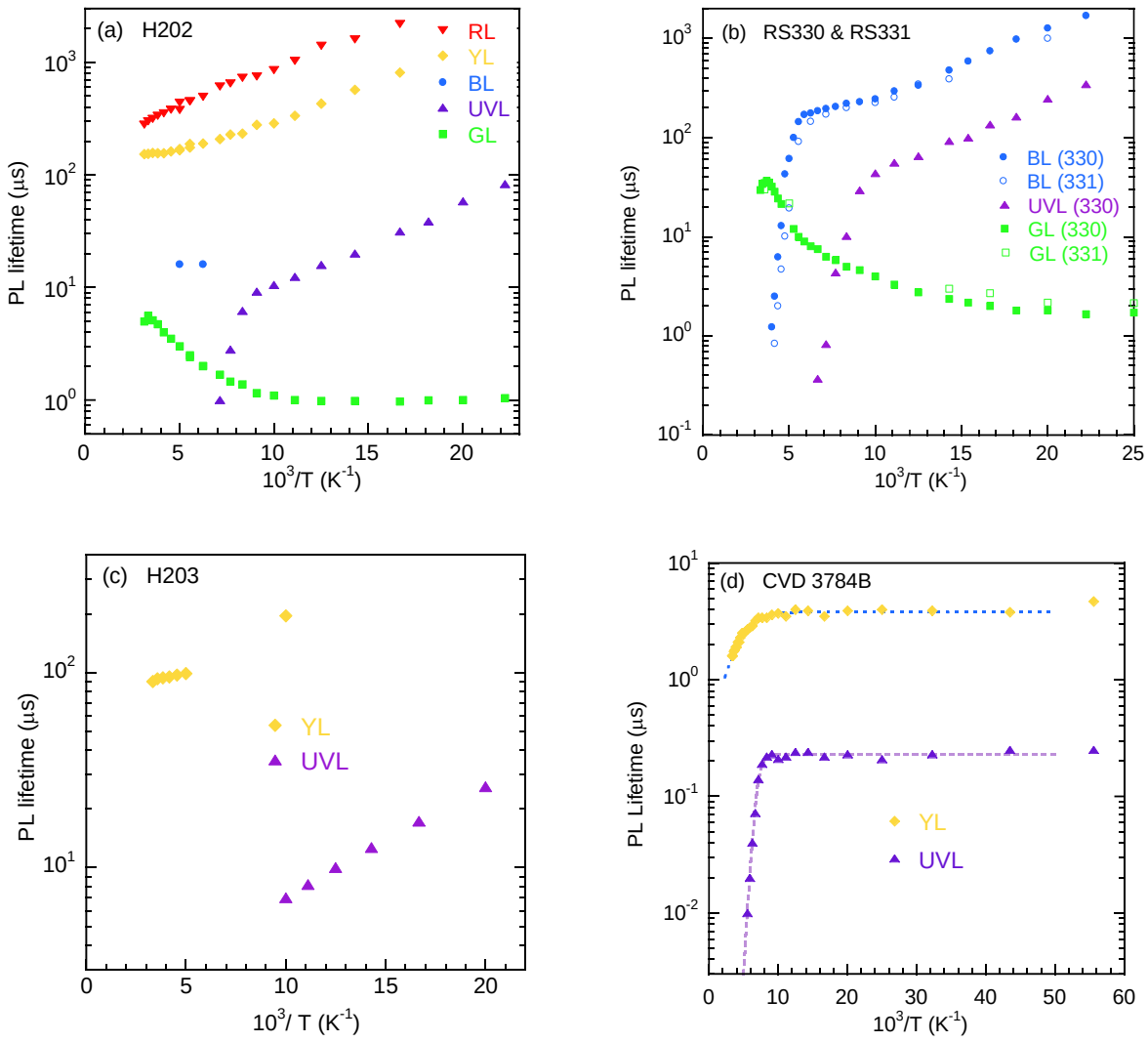

FIG. 4.14: (**a-c**) Temperature dependence of PL lifetime for undoped GaN samples H202, H203, RS330, and RS331. (**d**) Temperature dependence of the PL lifetime in a degenerate Si-doped GaN sample CVD 3784B. The dotted line for the UVL data is determined using Eq. (4.3) and the following parameters: E_A = 165 meV, C_{pA} = 10^{-6} cm^3/s and τ_0 = 0.23 μs. The YL band is fit using a simple decaying exponential where E_A = 50 meV, and τ_0 = 3.8 μs.

All the bands except the GL1 show a temperature dependence on n according to Eq.(4.5). It is important to note that for T < 40 K, the PL decay after a laser pulse is non-exponential for the RL1, YL1, BL1 and UVL bands, and has a power dependence of about -1. This is expected for DAP transitions, and is confirmed by the fact that the PL decay becomes exponential for T > 40 K as transitions originate from the conduction band. Conversely, in degenerate Si-doped GaN, the $n(T)$ dependence of the lifetime at low temperatures is not observed. The data for sample

cvd3784B is shown in FIG. 4.14(d), and the independence of temperature for *n* can be seen by virtue of the fact that the lifetime does not vary at all at low temperatures. This also confirms that the electron capture coefficient is independent of temperature. The lifetime of the UVL band as a function of temperature in FIG. 4.14(d) is fit by Eq.(4.3). The temperature dependence of the YL band is fit with a simple exponentially decaying function, but the activation energy as given by the slope of the fit has uncertain meaning.

4.8 Determining the concentration of free electrons

In conducting solids, placed in such a way that the current flow through them is perpendicular to an external magnetic field, the flow of charges will experience a Lorentz force propelling them to either side of the conductor depending on the sign of the charge. This produces a voltage difference across the conductor which is perpendicular to both the electrical current and the magnetic field. This effect, known as the Hall effect, was discovered in 1879 by Edwin Hall.[56] The potential difference across the sample which is being acted upon by an external magnet is the Hall voltage. Hall effect measurements are able to determine the concentration of free carriers in a semiconductor sample and the associated temperature dependence. In GaN grown by HVPE, there may be the presence of a degenerate layer located near the interface of the GaN and sapphire substrate which shunts the conductivity. At temperatures below 100 K, this layer is the main contributor of free electrons for the entire layer in the Hall effect measurements, and leads to erroneous estimations of the concentrations of free electrons as a function of temperature. A correction developed by Look called the two-layer model, may be applied to account for this degenerate layer.[57,58]

The concentration of free electrons and mobility for several HVPE GaN samples were measured by the temperature dependent Hall effect, and the results of a representative sample

(2015) are shown in FIG. 4.15. The data are corrected using the two layer model, and the temperature dependence of free electrons can be fit using the following expression:[57]

$$n = \frac{1}{2}\left[\sqrt{(\phi + N_A)^2 + 4\phi(N_D - N_A)} - (\phi + N_A)\right] \tag{4.6}$$

Here, $\phi = N_C^{'} T^{3/2} g^{-1} \exp(-E_D / kT)$ where g is the degeneracy of the donor state (g = 2), $N_C^{'}$ is the effective density of states in the conduction band at T = 1 K ($N_C^{'} \approx 5\times10^{14}$ cm^{-3} for $m^* = 0.22m_0$), N_D and N_A are the concentrations of shallow donors and acceptors, respectively, and E_D is the donor activation energy.

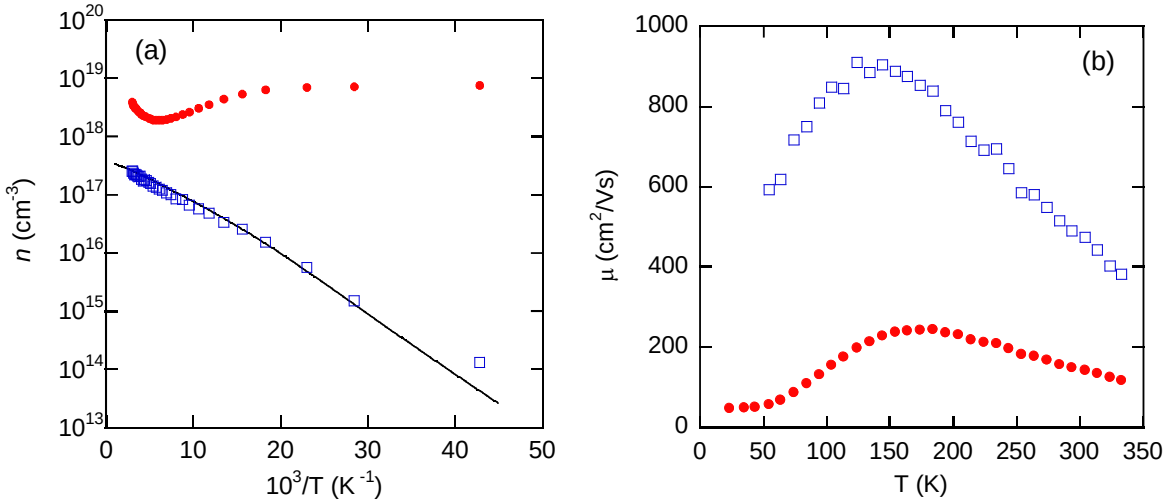

FIG. 4.15: Hall effect data for the concentration of (*a*) free electrons, *n*, and (*b*) mobility, μ, for T = 30 – 330 K. Sample is HVPE grown GaN (2015). The filled circles are the measured values and the empty squares are the corrected values from the two layer model. Parameters used for the corrected data are μ = (43.5±5.0) cm^2/Vs and $n = 2\times10^{20}$ cm^{-3} for the degenerate interface layer, where d = 24 μm is the total GaN thickness. In (*a*), the solid line is fit using $N_D = 4\times10^{17}$ cm^{-3}, $N_A = 5\times10^{16}$ cm^{-3}, and E_D = 17 meV.[59]

The value of N_A for this sample is estimated as 5×10^{16} cm^{-3} from the similarity in the temperature dependence of the electron mobility to the data presented in Ref. 57. To determine the concentration of shallow donors the data are fit, shown by the solid line in FIG. 4.15, and N_D = 4×10^{17} cm^{-3} with E_D = 17 meV.

The temperature dependence of free electrons was determined for several samples, and the two-layer correction was applied to those which were affected by the degenerate shunting region. The data for these calculations are shown in Table 4.2.

Table 4.2: Values of GaN samples for the concentrations of free electrons, n, and the PL lifetime, τ, for the UVL1, BL1, GL1, YL1, and RL1 bands.

Sample number	Thickness (μm)	n (10^{16} cm^{-3})			τ (μs)				
					UVL	BL1	YL1	RL1	GL1
		100K	180K	250K	100 K	180 K	180 K	180 K	250 K
104	10.6	2.1	4.6	6	11	20	175	400	4.5
201	15.3	6.8	14	18	8	23	120	290	3
202	20.4	2.3	4.8	6.1	10		180	450	4.3
203	21	3.4	7.4	9.4	7	18	100		
1007	22	1.8	3.6	4.3	20	55	320	950	9
2057	24	2.2	4.5	5.4	9.5		155	360	4
RS280	27	1.6 [a)]	13 [a)]	29 [a)]	100	390			49
B73	200	0.83	1.3	1.4	63	220			30

[a)] The two-layer model resulted in an unreasonable temperature dependence of n in sample RS280.

Included in Table 4.2 are the values for the thicknesses of the samples and the measured PL lifetimes for specifically the UVL, BL1, GL1, YL1 and RL1 bands. As can be seen from Table 4.2, a large number of samples have been investigated which are unintentionally doped or Si-doped GaN layers. A majority of the undoped GaN samples were grown by HVPE at Nitride Crystals, Inc. The thicknesses of the samples ranged from 3 to 30 μm, with the exception of a freestanding undoped GaN sample (B73) whose thickness is 200 μm and which was grown by HVPE at the Samsung Advanced Institute of Technology.

4.9 Electron capture coefficients

From Eq. (4.5), electron capture coefficients, $C_{n,A}$, for PL bands can be determined if n and τ_0 are measured experimentally by Hall effect and PL measurements, respectively. The values in Table 4.2 provide the means to calculate the capture coefficients. This works well for

the UVL band since it is present in each sample that was studied, and the capture coefficient for the UVL band, $C_{n,UVL}$, is given in Table 4.3. However, for other samples with unknown concentrations of free electrons, an alternative method can be used. Since the UVL band is ubiquitous in all the measured samples and $C_{n,UVL}$ is reliably determined from numerous measurements, the ratio of the PL lifetime for any band to the UVL lifetime, τ_A / τ_{UVL}, at T = 100 K can be used to determine the capture coefficient [Eq. (4.5)]. The capture coefficients for the BL1, YL1 and RL1 bands are determined by this method and listed in Table 4.3. Note that for the GL1 band, the lifetime at 250 K instead of 100 K was used, because both τ and $C_{n,A}$ have a strong temperature dependence at T > 100 K. The lifetime at 250 K and the temperature dependence of n for nine samples give the value of $C_{n,GL1} = (4\pm1)\times10^{-12}$. However, if a larger set of eighteen samples is analyzed using the ratio of the GL1 lifetime to UVL lifetime and Eq. (4.5), the ratio yields $\tau_{GL1}(250\,\mathrm{K}) / \tau_{UVL}(100K) = 0.455 \pm 0.022$ and the associated capture coefficient is $(6.6\pm1.1)\times10^{-12}$ cm^3/s. In the above estimations which use n, most of the error originates from the uncertainty in the determination of the concentration of free electrons. Incidentally, the values for τ_0 calculated from Eq.(4.5) agree well with the experimentally determined PL lifetimes, and thus we conclude that $C_{n,A}$ is constant for the range of temperatures used in the experiment. The capture coefficient of GL1 is the exception. The range of temperatures for which the coefficients are constant are given in Table 4.3. However, for some samples, the capture coefficients for YL1 and RL1 exhibited a weak temperature dependence, and the reason for this is not yet understood.

Furthermore, if the temperature dependence of the PL lifetime is measured, and the capture coefficient is measured for a particular band using another sample, the temperature dependence of the concentration of free electrons can be determined. This method is useful

especially for samples which have a heavy contribution from a degenerate region to the total electrical conductivity and give unrealistic values of *n*.

Table 4.3: Capture coefficients for PL bands, C_{nA}, where A represents the given band. $C_{n,UVL}$ is determined from lifetime and hall effect measurements, and the rest are determined from the ratio of the given PL band lifetime to UVL lifetime at 100 K (except GL1 which is measured at 250 K). The range of temperatures for which $C_{n,A}$ is constant is given.

	UVL	**BL1**	**GL1**	**YL1**	**RL1**
$C_{n,A}$ **(cm^3/s)**	$(3.0\pm0.5)\times10^{-12}$	$(6\pm1)\times10^{-13}$	$(6.6\pm1.1)\times10^{-12}$	$(1.0\pm0.2)\times10^{-13}$	$(4\pm1)\times10^{-14}$
τ_A / τ_{UVL}	-	4.64 ± 0.12	0.455 ± 0.022	29.9 ± 1.1	74.4 ± 2.3
Constant for *T*	~ 40-100 K	~ 40-180 K	-	~ 50-300 K	~ 50-300 K

For example, sample RS280 showed an unexpected temperature dependence of *n* where the concentration increased from 1.6×10^{16} cm^{-3} to 2.9×10^{17} cm^{-3} as the temperature increased from 100 to 250 K by using the two-layer model for the Hall effect measurements. At room temperature, the value is $n = 1\times10^{18}$ cm^{-3}. In contrast, the value of the concentration of electrons calculated from PL lifetime values is below 10^{16} cm^{-3} at room temperature, the lowest value for any sample measured. To obtain this value of the free electron concentration, the electron capture coefficients for the UVL (at T = 100 K), BL1 (at T = 180 K) and GL1 (at T = 250 K) bands were used.

In conclusion, the PL lifetimes for many samples were measured and, in conjunction with the temperature dependence of free electrons obtained from Hall effect data, were used to determine electron capture coefficients for several defect related bands. Conversely, if the capture coefficients are previously determined through other means, the temperature dependence of *n* can be determined. Additionally the presence of a degenerate layer near the sapphire interface is confirmed.

Chapter 5: Green luminescence in undoped GaN

Green luminescence observed in undoped, high purity GaN samples grown by HVPE is perhaps the most interesting band studied yet. There are several interesting features about the GL behavior which lead to important conclusions and theories. In particular the decay of the GL is exponential at any temperature above 30 K which points to the fact that it is most likely caused by an internal transition between an excited state and ground state of the same defect. Additionally, the lifetime of the GL increases with increasing temperature, which is the only band in undoped GaN to do so. These interesting behaviors are explained here. The GaN layers for this chapter ranged in thicknesses of 10 – 30 μm, and were deposited on *c*-plane sapphire substrates. The room temperature concentration of electrons is from 2×10^{16} to 4×10^{17} cm^{-3} as determined from temperature dependent Hall effect measurements.

5.1 Exponential decay of GL at low and high temperature

In FIG. 5.1, the logarithm of the GL intensity is plotted as a function of time. Interestingly, the decay is almost exponential at any temperature. The non-exponential tail of the PL decay can be attributed to contributions from the less intense and longer decaying YL band. With increasing temperature, the GL intensity becomes higher than the YL, and the tail disappears. The nature of the YL can be confirmed by plotting the TRPL spectra. Typically, defect related PL decays non-exponentially for temperatures below 50 K. At these temperatures, DAP recombination dominates since most electrons are frozen at the donor levels, and the nature

of recombination is affected by the Coulomb interaction between the pairs as well as the statistical processes associated with charge capture and recombination. Thus, the decay is non-exponential for $T < 50$ K. With increasing temperature, electrons are thermally emitted to the conduction band, and transitions between the conduction band and defect levels have exponential behavior. A PL band which has exponentially decaying behavior at any temperature, such as the GL band, signifies that the transition is most likely an internal transition between an excited state of the defect and a ground state.

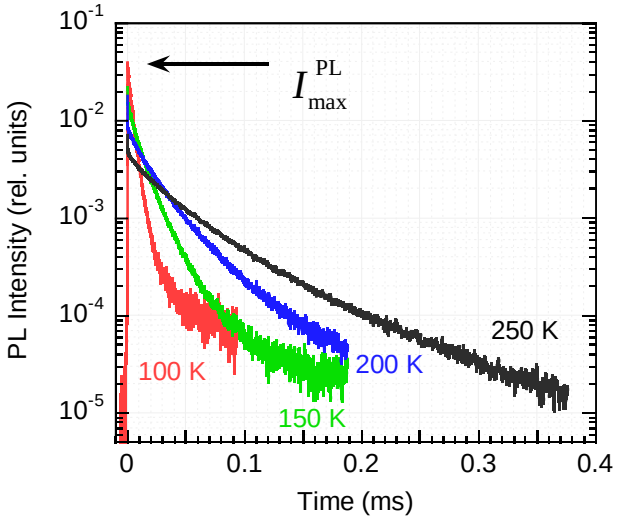

FIG. 5.1: The decay of the PL intensity is plotted on log-linear scale for the temperatures 100, 150, 200, and 250 K. The decay is nearly exponential at any temperature, since the non-exponential tail can be attributed to the YL band. $I_{\max}^{PL}$ is defined as the point where the slow decay begins; *i.e.*, after the fast excitonic decay contribution.

5.2 Unusual temperature dependence of GL lifetime

In HVPE grown undoped GaN, the PL lifetime, τ, for most defect-related bands is undetermined for $T < 30$ K, and decreases with increasing temperature in accordance with the thermal quenching. This behavior is seen for the lifetime of the defect related bands (except GL1) in Section 4.7 and FIG. 4.14 and can be fit by the previously derived relationship:

$$\tau^{-1} = C_{nA} n \,. \tag{5.1}$$

Here, C_{nA} is the electron capture coefficient for the acceptor associated with the PL transitions, The capture coefficient is a defect specific parameter which is given as the product of the electron capture cross section, σ_{nA}, and the mean thermal velocity of electrons in the conduction band, $\langle v_n \rangle$:

$$C_{nA} = \langle v_n \rangle \sigma_{nA} . \tag{5.2}$$

For most defect related PL bands, the PL lifetime decreases with increasing temperature, as the concentration of free electrons increases with temperature. However, this is not the case for the GL band. For temperatures below T = 100 K for undoped GaN samples H201 and 1412, and Bulk sample 73, the lifetime decreases slightly with an activation energy of 2 meV (for unknown reasons), and is independent of n; *i.e.*, the lifetime at low temperatures is sample independent. The following empirical relationship was derived to fit the GL lifetime at low temperatures and is shown for H201 in FIG. 5.2: [60]

$$\tau(T) \approx \tau_2 = \tau_{20} \exp(E_2 / kT) \tag{5.3}$$

where $\tau_{20} = 0.67\,\mu s$ and $E_2 = 2\,meV$. The fact that the PL lifetime is independent of the concentration of free electrons at low temperatures helps to confirm the assumption that the GL is caused by an internal transition between an excited state of a defect and the ground state of the same defect. [60] As opposed to every other measured PL band in GaN, the lifetime of the GL begins to increase with increasing temperature after a specific temperature.

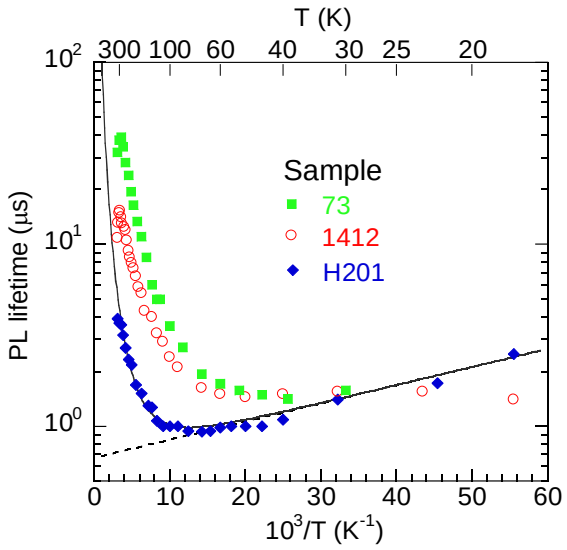

FIG. 5.2: lifetime as a function of temperature for the GL band in undoped GaN samples H201 and 1412, and bulk GaN sample #73. The GL data for H201 are fit with the dependence $\tau(T) = \tau_1 + \tau_2$ from Eqs. (5.3) and (5.4), with the parameters $a = 2.8$ and $\tau_1(100\text{ K}) = 0.17$ μs, $\tau_{20} = 0.67$ μs, and $E_2 = 2$ meV. The low temperature portion of the GL data is fit by Eq. (5.3).

The lifetime begins to increase at 100 K for sample H201, and above $T > 50$ K for samples 1412 and 73 (FIG. 5.2). The high-temperature portion of the PL lifetime, τ_1, for sample H201 can be empirically fit by the equation:[60]

$$\tau(T) \approx \tau_1 = \tau_1(100K)\left(\frac{T}{100K}\right)^a . \qquad (5.4)$$

In this expression, $\tau_1(100K) = 0.17$ μs and $a = 3.1$ for sample H201. Interestingly, Eq.(5.1) still applies to these data, where the lifetime is inversely proportional to the concentration of free electrons. Intuitively, an increase in the concentration of free electrons should cause a decrease in the measured lifetime. However, Eq.(5.1) also contains the parameter C_{nA} which surprisingly has a stronger effect on the measured lifetime and dictates the lifetime at higher temperatures. Specifically, C_{nA} has a strong temperature dependence, although this is unusual for defects participating in radiative recombination. If the temperature dependent Hall effect data for the

samples are used together with the measured PL lifetime, the capture coefficient as a function of temperature can be calculated. This is shown in FIG. 5.3. As can be clearly seen, C_{nA} decreases by two orders of magnitude with increasing temperature. The dependences for three samples are shown and can be fit using a power law of the form [60]

$$C_{nA}(T) = C_{nA}(100K)\left(\frac{100K}{T}\right)^{b}. \tag{5.5}$$

Here, $C_{nA}(100K) = 3 \times 10^{-11}$ cm^3/s for samples 1007 and 73 (lines 1 and 2, respectively), and is equal to 2.3×10^{-11} cm^3/s for sample RS280 (line 3). The parameter b = 2.5, 3.0, and 3.3 for the lines 1, 2, and 3, respectively. From Eq. (5.5), it can be seen that the C_{nA} data decrease proportionally to T^{-b} with $b \approx 3$. This inverse cubic temperature dependence is characteristic of involving an attractive center, and is very similar to that of the electron capture cross section of giant traps.[10, 61]

Interestingly, giant traps have previously only been probed by photoconductivity experiments of the lifetimes in Si and Ge, and they are speculated to involve non-radiative transitions. Giant traps are attractive centers in semiconductors with large capture cross sections for electrons and holes on the order of $10^2 - 10^4$ nm^2 at liquid He temperatures.[10, 62, 63] The capture cross section is temperature dependent since carriers can be thermally ejected back into the conduction band with increasing temperature. The actual trap itself has Coulomb excited states similar to a hydrogen atom, and after capture, the electrons transition through the excited states to the lowest level releasing energy via single phonon emission. This is called cascade capture and was postulated by Lax and other researchers in the 1960's. The characteristic feature of giant traps is their inverse cubic temperature dependence of the capture cross section. Thus, it was surprising that the GL capture coefficient, and consequently the capture cross section [Eq.

(5.2)], behaves as a non-radiative giant trap. Typically, radiative transitions involve capture coefficients which are independent of temperature. In order to explain the unusual behavior, the following model was developed involving an attractive center with an excited state near the conduction band and a corresponding lifetime composed of a two-step process. [60]

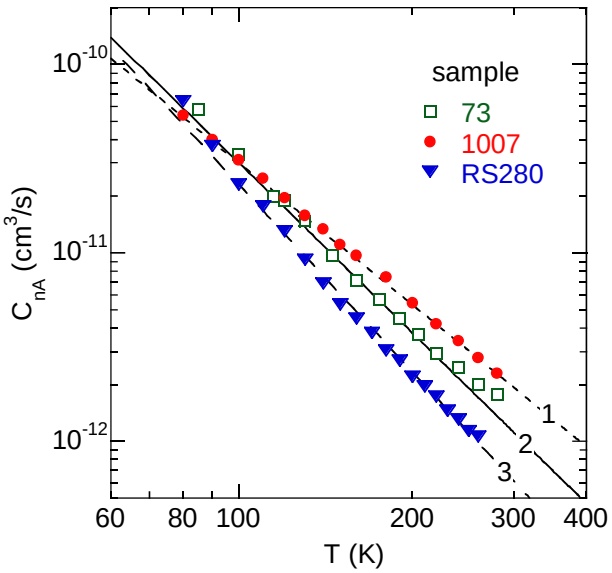

FIG. 5.3: The dependence of temperature for the electron capture coefficient for the GL band in undoped GaN samples 1007 and RS280 and bulk GaN sample 73. The data are fit using Eq. (5.5) and with C_{nA} (100 K) = 3×10^{-11} cm^{-3}/s, for lines 1 and 2, and 2.3×10^{-11} cm^{-3}/s, for line 3. The parameter b in Eq. (5.5) is equal to 2.5, 3.0, and 3.3, for lines 1-3, respectively. Reprinted with permission from Reshchikov *et al.*, Phys. Rev. B **93**, 081202(R) (2016). ©2016 American Physical Society. [60]

In our model, the attractive defect center has two transition levels in the bandgap, such as in the case of the theorized C_N defect. Under above-bandgap illumination, a hole is first captured by the C_N defect at the -/0 transition level. Electronic transitions from the conduction band to this level are presumably the cause of a yellow luminescence band in undoped GaN, but this remains under question. With increasing excitation intensity, the GL band emerges in PL measurements with a super-linear dependence on excitation intensity. Within this model, the defect must capture two holes to produce GL in order to explain the GL excitation intensity dependence.

Thus, the C_N defect captures two holes, and the 0/+ transition level becomes active. Simultaneously, it is predicted that the C_N defect has an excited state located close to the conduction band. The GL is then caused by an internal transition between these two states, which is consistent with the exponential PL decay at low temperatures.

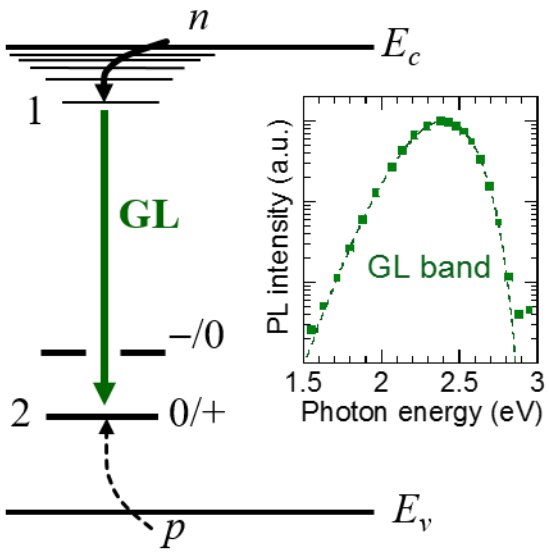

FIG. 5.4: Diagram of electron transitions associated with the GL band and shape of GL band at 30 K (inset). The attractive center is able to capture two holes, and becomes the positively charged 0/+ transition level after the second capture (shown by a dashed arrow from the valence band). To produce GL, an electron is first captured non-radiatively by the excited state (level 1) and cascades down by the Lax mechanism to a lower energy level. An internal transition from level 1 to level 2 causes the GL. Since the PL lifetime is governed by these two additive processes, the longer of the two lifetimes will determine the measured PL lifetime. Reprinted with permission from Reshchikov *et al.*, Phys. Rev. B **93**, 081202(R) (2016). ©2016 American Physical Society. [60]

The remaining piece in the puzzle is the unusual temperature dependence of the PL lifetime which may now be explained by assuming that the excited state of the associated defect (level 1 in FIG. 5.4) behaves as a giant trap. If this is indeed the case, electrons will be captured by this giant trap and transition non-radiatively through the ladder of excited states to level 1, before they recombine radiatively with one of the bound holes at level 2 (FIG. 5.4). These two processes will both have related lifetimes, and the measured lifetime is then the sum of these two

processes. The temperature dependence of the lifetime will be simply $\tau(T) = \tau_1 + \tau_2$, where τ_1, given by Eq. (5.4) is the high temperature portion and is dependent on the electron capture by the giant trap. This lifetime has an inverse cubic temperature dependence. The second lifetime, τ_2, is the low temperature portion of $\tau(T)$ and is given by Eq. (5.4). This lifetime is the waiting time for an electron at the bottom of level 1 to recombine with a bound hole at level 2. From the data in FIG. 5.2 and the calculated dependencies from Eqs. (5.4) and (5.5), it can be seen that the PL lifetime is dictated by τ_2 at low temperatures, and by τ_1 and the cascade capture of electrons by the giant trap at high temperatures. Typically, lifetimes of radiative PL bands have inverse relationships due to the competing nature of available channels for recombination. In the case of GL, however, the lifetime is an additive process.

An analytical expression can be developed for the decay of the PL intensity as a function of time, taking into account the additive lifetimes. Let us assume that N_A^+ is the total concentration of attractive centers with two bound holes and either an electron in the excited state (level 1) which we will label N_1^+, or without an electron in the excited state which we label N_2^+, so that $N_A^+ = N_1^+ + N_2^+$. We may use the C_N defect as an example. After the laser pulse, the concentration of N_A^+ will decay in time as electrons from level 1 recombine at level 2. This is an internal transition and is governed by the lifetime τ_2. We can describe the change in the concentration of N_A^+ by the relationship,

$$\frac{dN_A^+}{dt} = -\frac{N_1^+}{\tau_2}. \tag{5.6}$$

The concentration of defects with two bound holes and an electron in the excited state will be reduced as electrons recombine with a bound hole in the ground state, and the concentration will increase as electrons are captured non-radiatively by the giant trap-like excited state. Thus,

$$\frac{dN_1^+}{dt} = \frac{N_2^+}{\tau_1} - \frac{N_1^+}{\tau_2}. \tag{5.7}$$

By solving this system of equations, an analytical expression for the decay of the PL intensity as a function of time is derived and given as, [60]

$$I^{PL}(t) = \frac{N_A^+(0)}{\tau_1 - \tau_2}\left(e^{-\frac{t}{\tau_1}} - e^{-\frac{t}{\tau_2}}\right) = I^{PL}(0)\left(e^{-\frac{t}{\tau_1}} - e^{-\frac{t}{\tau_2}}\right). \tag{5.8}$$

In this expression, $N_A^+(0)$ is the concentration of the center with two bound holes immediately after a laser pulse has saturated the -/0 level of the C_N defect with holes. We define $I^{PL}(0)$ as the initial value of the slow component of the PL intensity immediately after a laser pulse. This is shown on FIG. 5.1 and is labeled as $I_{\max}^{PL}$. From Eq. (5.8), the PL intensity will be dictated by the one of the two lifetimes for low and high temperatures. At low temperatures, the cascade capture of electrons will be very fast such that $\tau_1 << \tau_2$ and Eq. (5.8) will be approximately $I^{PL}(t) \approx I^{PL}(0)\exp(-t/\tau_2)$, and thus governed by the lifetime of the internal transition. At high temperatures, the excited state, level 1, will thermally eject electrons to the conduction band and the lifetime for an electron to become available for internal recombination will become longer with increasing temperature. In this case, $\tau_1 >> \tau_2$, and Eq. (5.8) will be governed by the lifetime of the electron in the giant trap. From this, we conclude that the measured PL lifetime will be determined by the longer of the two individual lifetimes, since the measured PL lifetime

as a function of temperature is given as the sum of τ_1 and τ_2. This is experimentally verified by fitting the data in FIG. 5.2 as the sum of Eqs. (5.3) and (5.4).

Eq. (5.8) provides predictions for the values of $I_{\max}^{PL}$ as a function of temperature. FIG. 5.5 shows the predicted (solid line) and experimentally determined values of $I_{\max}^{PL}$ (squares) as a function of temperature. Additionally the temperature dependence of the lifetime (triangles) is shown for comparison. The decrease in $I_{\max}^{PL}$ for $T > 40$ K is both predicted and seen experimentally, and occurs concurrently with the increase in the PL lifetime, as a result of $\tau \approx \tau_1$.

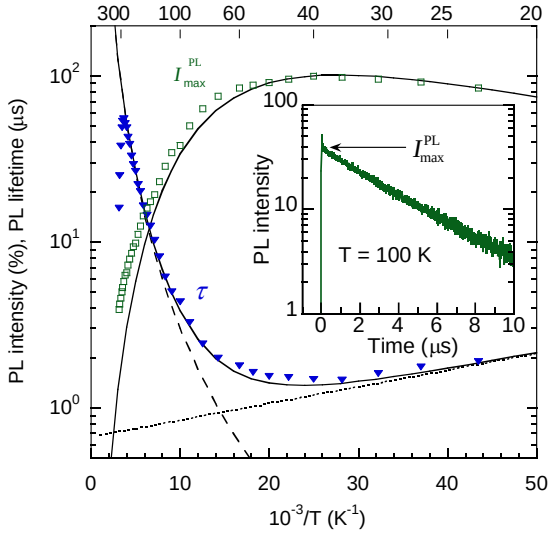

FIG. 5.5: PL lifetime (triangles) and PL intensity maximum after a laser pulse, $I_{\max}^{PL}$, (squares) as a function of temperature, for the GL band in GaN sample RS280. The fits for $I_{\max}^{PL}(T)$ and $\tau(T) = \tau_1 + \tau_2$ are calculated from Eqs. (5.3), (5.4), and Eq. (5.8) using the same parameters given in the caption of FIG. 5.2. The parameters τ_1 and τ_2 from $\tau(T)$ are shown as dashed and dotted lines, respectively. The measured and calculated dependences of $I_{\max}^{PL}$ (T) are normalized to 100% at 40 K. The GL decay kinetics at 500 nm are shown in the inset for 100 K. Reprinted with permission from Reshchikov et al., Phys. Rev. B **93**, 081202(R) (2016). © 2016 American Physical Society.[60]

The capture cross section of the attractive center, supposedly C_N, at various temperatures can be calculated for our measurements, and is estimated as $\sigma_{nA} \approx 3\times10^{-18}$ cm^2 at $T = 100$ K, and

$\sigma_{nA} \approx 10^{-19}$ cm^2 at T = 300 K. Although the original values of the giant trap cross sections were at least two orders of magnitude larger (between 10^{-17} and 10^{-14} cm^2 at T = 300 K), these values were measured for defects in Si and Ge. Furthermore, photoconductivity methods were used to measure the lifetimes and from this to estimate the capture cross sections. In this way, the lifetime of the escape of the electron from the giant trap to the conduction band is measured, as opposed to our methods which measure the waiting time of the electron in the excited state before it internally recombines at the ground state. This may be the cause of the discrepancy in the capture cross section values.

In summary, the lifetime of the GL in undoped high purity GaN grown by HVPE is significantly different and demonstrates interesting behavior as opposed to other PL bands in the same samples. Specifically, the lifetime increases dramatically with increasing temperature, and is characteristic of being caused by an attractive center. Additionally, the PL decay at any temperature is independent of temperature, which indicates that the related transitions are internal transitions. Furthermore, the lifetime of the PL can be described by two processes which collectively contribute to the measured dependences with greater value at low and high temperature, such that one lifetime will dominate over the other depending on the temperature. The capture coefficient and thus the electron capture cross section of the related defect has an inverse cubic temperature dependence which is surprisingly similar to the capture cross section of giant traps observed in Si and Ge. We explain this model by suggesting that an attractive center with two transition levels in the bandgap, such as the C_N defect, captures two holes after a laser pulse, and simultaneously creates an excited state near the conduction band. This excited state behaves like a giant trap. Internal PL transitions occur between this excited state and the ground state of the attractive center, and the lifetime is the sum of the electron waiting time in

the giant trap-like excited state, and the time of recombination of the electron with a bound hole at the 0/+ transition level of the attractive center.

Chapter 6: Luminescence in Mg-doped GaN

Magnesium is considered to be the only viable impurity for obtaining *p*-type conductivity in GaN. During HVPE or MOCVD growth of Mg-doped GaN, the Mg_{Ga} defect is introduced as a shallow acceptor[64,65,66] with an ionization energy of ~ 200 meV. [67,68] In Mg-doped GaN, self-compensation can make it difficult to obtain reliable *p*-type conductivity. Hydrogen during growth passivates the Mg forming complexes instead of optically active defects, yet H also causes the Fermi level to be shifted away from the valence band which allows for incorporation of Mg.[69] With increasing concentration of Mg, the room temperature concentration of holes increases until about 10^{18} cm^{-3}, which corresponds to a Mg concentration of 3×10^{19} cm^{-3}, and beyond this point, the hole concentration decreases with a further increase in Mg.[70] Luminescence studies on Mg-doped GaN provide basic information on the defect properties and the nature of the transitions. In this chapter, we briefly discuss the effect of temperature and excitation intensity on the SSPL and the effect of both of these on the time delay of the UVL and BL bands in heavily doped, GaN:Mg.

6.1 Effect of excitation intensity on GaN:Mg

The Mg-doped GaN sample (R2-1840) used for this work was grown at Nitride Crystals by HVPE, on c-plane sapphire. The total thickness of the layer is 4.7 μm, with n-type GaN as the first layer (3.7 μm), and a Mg-doped *p*-type layer (1 μm) as the top layer. The samples did not receive any post-growth annealing, although annealing is necessary in MOCVD growth to

activate the Mg acceptors. The flow of NH_3 in the HVPE growth was lower than typical values for MOCVD grown samples, and *p*-type conductivity was obtained without annealing.

The steady-state PL spectra taken at T = 18 K for various excitation intensities are shown in FIG. 6.1. For high excitation intensities of P_{exc} = 0.2 W/cm^2, the UVL band completely dominates in the spectrum, and conceals a faint BL band as its shoulder. As the excitation intensity is reduced, the BL band emerges, and is comparable in intensity to the UVL band at P_{exc} = 0.03 mW/cm^2. Both the UVL and the BL bands are assumed to be caused by transitions to the Mg_{Ga} acceptor. From the shape of the UVL band and a peak shift of 20 meV of the ZPL with increasing excitation intensity, it can be attributed to transitions from a shallow donor (low temperature) or the conduction band (high temperature) to the Mg_{Ga} acceptor.

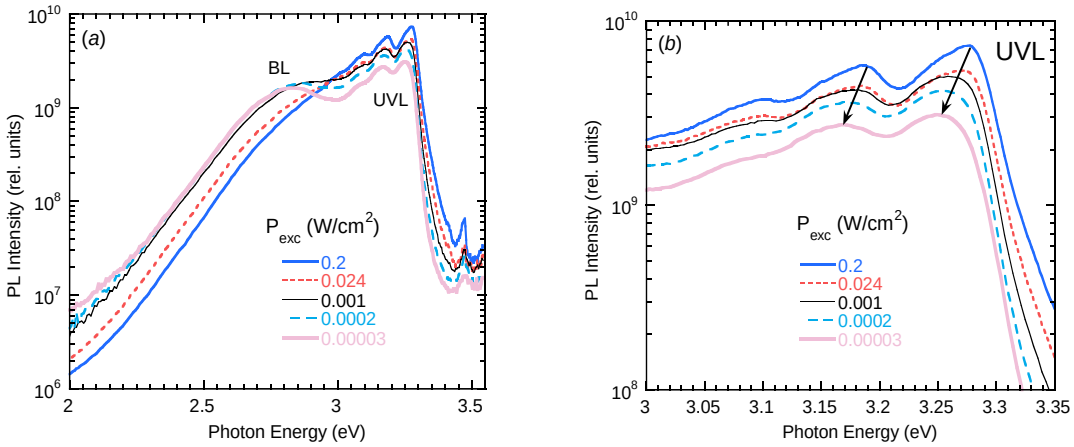

FIG. 6.1: (**a**) SSPL spectra for *p*-type Mg-doped GaN sample R2-1840, for T = 18 K, and P_{exc} = 2.8×10^{-7} – 0.2 W/cm^2. The UVL band is seen for the whole range of excitation intensities, and the BL band is seen for P_{exc} < 0.001 W/cm^2 since the BL-related acceptor becomes saturated with photo-generated holes above these excitation intensities. (**b**) A zoomed-in region of the UVL peak shift with arrows indicating the peak shift.

The red-shift of the UVL band and its broadening with decreasing excitation intensity are well-studied and commonly reported,[31,71,72,73,74,75] and a shift of the BL peak typically on the order of 0.1 eV is reported in numerous works.[71,72,73,74,75,76,77] In FIG. 6.1, the peak of the BL in the SSPL spectra is difficult to observe since it is obscured by the UVL band until lower

excitation intensities, where the BL peak red shifts. If the spectra are measured at temperatures greater than 120 K, the UVL band quenches and reveals the BL band. This is seen in FIG. 6.2, where the UVL band at T = 130 K is only seen as a shoulder on the high energy side of the BL band at 0.2 W/cm^2. With increasing excitation intensity, the peak of the BL band blue-shifts by about 134 meV.

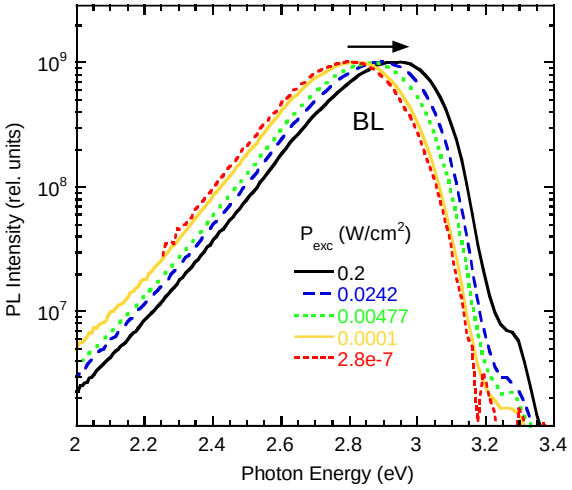

FIG. 6.2: SSPL of Mg-doped GaN sample R2-1840. The BL band is shown for P_{exc} = 0.2 – 2.8 ×10^{-7} W/cm^2 and T = 130 K. The total shift of the BL peak with increasing excitation intensity is 134 meV. The data are normalized.

The shift of the UVL band with increasing excitation intensity may be explained by either the presence of potential fluctuations or its DAP nature. [5,31] Potential fluctuations are present in samples with an inhomogeneous distribution of charged defects. Regions with a high density of impurities will cause a change in the potential landscape, where high concentrations of donors will cause valleys in the conduction band, and high concentrations of acceptors will cause hills in the valence band. Free electrons and holes under UV illumination are trapped in these valleys and hills, respectively. During low intensity illumination, recombinations will occur between the hills and the valleys, resulting in diagonal, lower energy transitions. With increasing excitation intensity, the potential fluctuations are flattened, and transitions will become vertical with a

higher emission energy. The sample used for these measurements is heavily compensated and has a high concentration of Mg impurities which would allow the presence of potential fluctuations, and may be able to explain the blue-shift of the UVL band with increasing excitation intensity. For the UVL band, it is most likely that the blue-shift is caused by potential fluctuations and not their DAP nature, although the UVL band originates from DAP transitions. This may be explained by the large blue-shift of the UVL band. If the shift was due to DAP nature, the amount by which the UVL band could shift should be less than half of the ionization energy of the shallow donor.[78] Since this is not the case, long range potential fluctuations may explain better the large shift.

On the other hand, the blue-shift of the BL band with excitation intensity may be a result of deep DAP transitions. [31] Recombinations which occur between distant pairs can occur with similar probability to transitions between close pairs, as long as the excitation intensity is relatively low. Distant pairs have small overlap of the wavefunctions, and transitions between them will have relatively long lifetimes. Close pairs, with greater overlap of the wavefunctions, will recombine faster. With increasing excitation intensity, the recombinations due to distant pairs will saturate since the close pairs will begin to recombine faster. Thus, the energy of emission will blue-shift with increasing excitation intensity as close pairs become the dominant contributor. The level of the donor is most likely deep, since the Coulomb interaction between the donor and acceptor pairs pushes the levels towards the edge of the bandgap,[79] and shallower levels would disappear into the conduction band.

6.2 Effect of temperature on the peak position of BL and UVL

Temperature has a similar effect on the peak position of the BL and the UVL bands. In FIG. 6.3, the red-shift of the BL band with increasing temperature is seen for P_{exc} = 0.2 W/cm^2.

The red-shift of the BL band with increasing temperature also hints to its deep DAP nature. The strong Coulomb interaction is expected to push the donor levels closer to the conduction band. With increasing temperature, the close pairs will lose their electrons as they are ionized to the conduction band, and the emission spectra will be a result of the remaining distant pairs, which have lower emission energy and are further from the conduction band, such that their electrons are not thermally emitted at the same temperature as the close pairs.

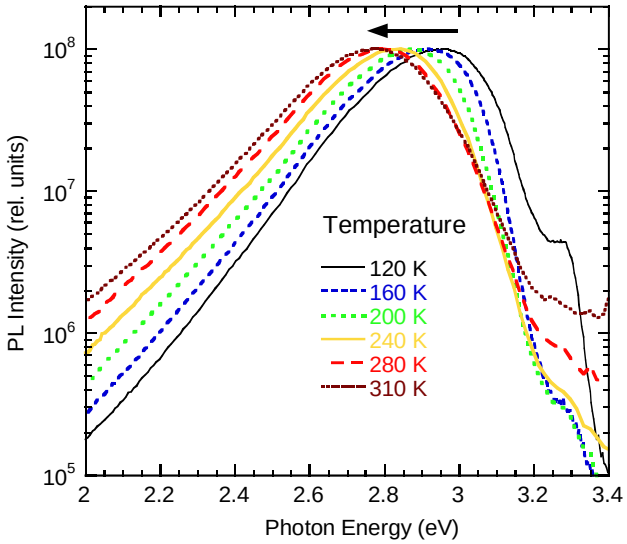

FIG. 6.3: SSPL of Mg-doped GaN sample R2-1840, with P_{exc} = 0.2 W/cm^2. The temperature increases from 120 to 310 K, and the corresponding peak shift is 174 meV to lower energies. The data are normalized.

In order to understand this effect, the temperature shift as a function of excitation intensity must also be analyzed. As can be seen in FIG. 6.4(a), the temperature-induced shift of the BL band peak for P_{exc} = 0.2 W/cm^2 is significant for the whole range of temperatures. At high excitation intensity and low temperature, the BL is a result of recombinations between close pairs. With increasing temperature, close pairs thermally emit their charges and distant pairs dominate the contribution to the BL. The large shift in the BL peak at high excitation intensity is due to recombination from closer pairs to more distant pairs. In contrast, the temperature-induced shift for P_{exc} = 0.00017 W/cm^2 is weakly dependent on temperature for T < 150 K, since distant

pairs contribute at low excitation intensity, and transform into more distant pairs at higher temperatures. The corresponding shift of the BL peak will not be as extreme at low excitation intensity. The same behavior is seen in FIG. 6.4(b). The BL peak shift as a function of excitation intensity is greater at lower temperatures, since the close pairs still can contribute at lower temperatures. The emission spectrum at low temperatures will show the contribution of the close pairs at high excitation intensity and the contribution of the distant pairs at low excitation intensities. With increasing temperatures, the close pairs will thermally emit the charges, leaving only the distant pairs to contribute to the spectrum, and the change in the peak position will not be as significant as it is at low temperatures.

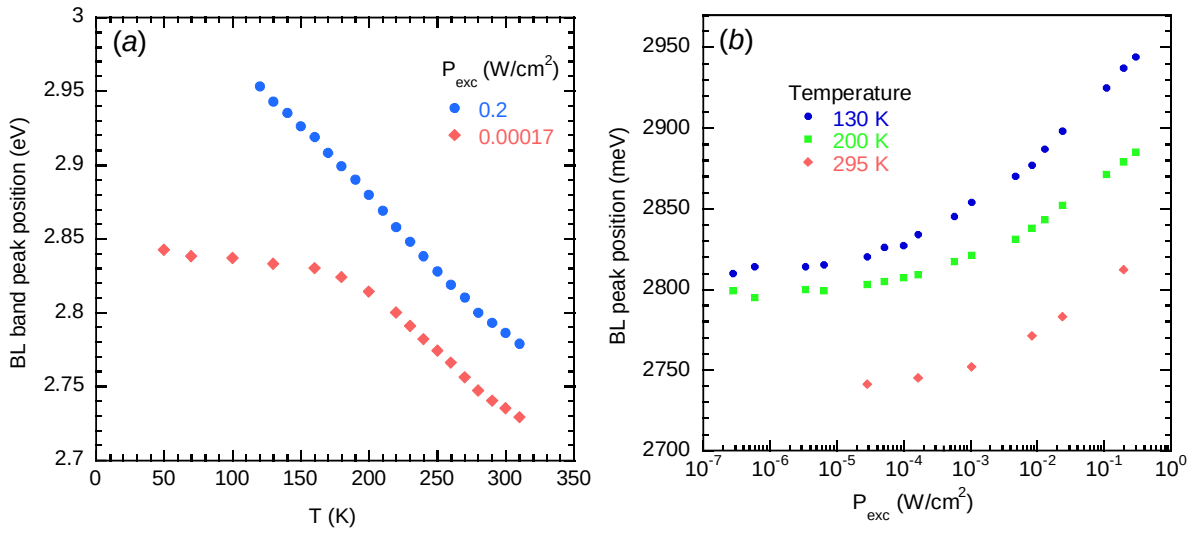

FIG. 6.4: The peak intensity of the BL band in Mg-doped GaN sample R2-1840. (***a***) the change of the BL peak position with increasing temperature and for P_{exc} = 0.00017 and 0.2 W/cm^2. (***b***) The dependence of the BL peak position on excitation intensity for T = 130, 200 and 295 K.

6.3 Effect of time-delay on the peak position of BL and UVL

TRPL can confirm the nature of the DAP transitions.[32] The peak position of the PL bands red-shifts with increasing time-delay, which signifies that close pairs (higher emission energy) contribute at fast time-delays and distant pairs (lower emission energy) contribute at longer time

delays. In TRPL measurements, both the BL and UVL bands can be clearly resolved, if they are measured at the optimal temperatures. In FIG. 6.5, the time-resolved spectra of the UVL band measured at T = 18 K are shown for time delays of 3×10^{-7} to 1×10^{-5} s. The lines from a SSPL spectrum for two excitation intensities are shown also on the graph and correspond to the shape measured in TRPL. The peak of the UVL band red-shifts with increasing time after the laser pulse by about 30 meV, but it is unclear whether the shift originates from potential fluctuations or from the DAP nature. At short time delays, close pairs will be the main contributor to the spectrum and will have higher transition energies. As time increases, distant pairs will begin to contribute with lower transition energies and a longer time-delay.

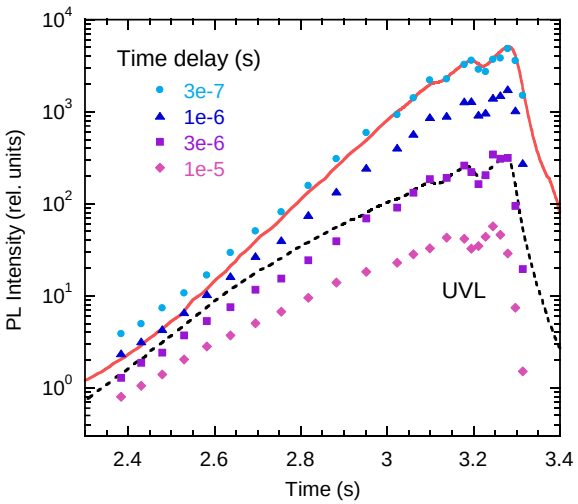

FIG. 6.5: TRPL spectra (symbols) of the UVL band for *p*-type Mg-doped GaN sample R2-1840, and for T = 18 K. N= 0.01.The spectra is measured for time delays of 0.3 to 30 μs after the laser pulse. The UVL band is most intense for short time delays. SSPL spectra are shown for comparison taken with P_{exc} = 0.2 (dotted line) and 100 W/cm^2 (solid line).

The same can be seen for the BL band in FIG. 6.6. Its red-shift with increasing time delay signifies that it arises from DAP transitions. This shift in the BL peak position is most likely due to a deep donor to shallow acceptor, since the strong Coulomb interaction between the deep-level pairs is sufficient to explain the red-shift of 80 meV. The shift of the BL peak with time-delay

has a temperature dependence as can be seen in FIG. 6.7 which again points to the nature of the deep-donor involved with the transition.

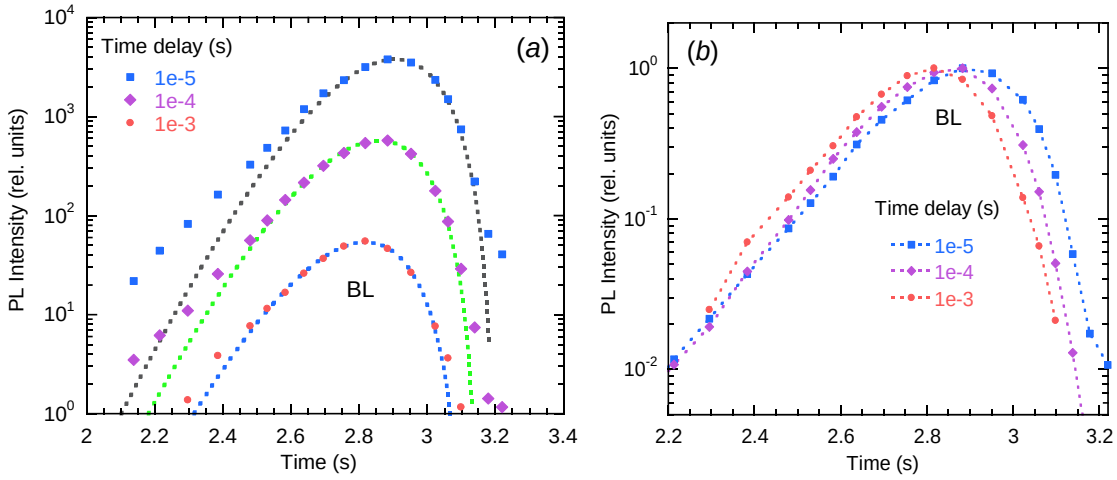

FIG. 6.6: (**a**) TRPL spectra of the BL band in *p*-type Mg-doped GaN sample R2-1840, and *T*= 130 K. With increasing time delay, the peak of the BL band red-shifts. (**b**) The data are normalized to the peak of the BL band.

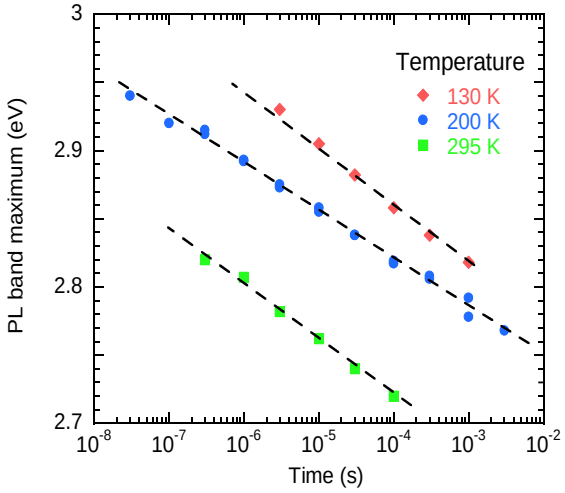

FIG. 6.7: BL peak dependence on time delay for *p*-type Mg-doped GaN sample R2-1840, **at** N = 0.01, and *T*= 130, 200, and 295 K. BL peak red-shifts with increasing time-delay.

In conclusion, the UVL and BL bands have been studied in Mg-doped GaN samples grown by HVPE. The shift of the peak position for the UVL band indicates the presence of potential fluctuations which may be expected in heavily compensated GaN. The same shift of the BL band however is attributed to DAP transitions between a deep donor and a shallow acceptor.

This may be deduced since with increasing temperature, the BL peak redshifts, signifying the thermal emission of close pairs, and the contribution resulting from distant pairs.

Chapter 7: Conclusions and Future Outlook

Understanding the behaviors of point defects in GaN as they pertain to PL measurements has been the goal of this work. The methods of TRPL and SSPL were used together to determine much useful information regarding the shape and position of unresolved PL bands, the PL lifetime of defect-related luminescence, capture coefficients of defects, and the concentrations of free electrons in the studied samples. Additionally, SSPL measurements are able to identify the nature of transitions such that DAP origins can be distinguished from eA transitions, and from TRPL measurements, external transitions are altogether differentiated from internal transitions between an excited state and ground state of the same defect.

Several major defect-related PL bands were studied in this work which are specifically the UVL, BL, GL, YL and RL bands. The samples studied were either high-purity undoped GaN layers grown by HVPE or GaN layers grown by MOCVD with varying doping levels. The lifetimes of these bands were investigated using TRPL measurements, and a theoretical consideration on the various lifetimes of electron and hole capture by defects was presented. The lifetimes of defect related luminescence ranged from 10 ns from a very fast RL3 band, to 1 ms for a much slower RL band. Average lifetimes were in the range of 10 μs to 1 ms for most of the defect-related PL bands.

The concentrations of free electrons were determined by obtaining the capture coefficients of defects from well-resolved PL measurements and from the measured PL lifetimes.

These values were compared with temperature dependent Hall effect data, and showed that in some samples, the presence of a degenerate layer near the GaN-sapphire interface produced erroneous results from the Hall effect data.

The lifetime of most defect-related bands decreases with increasing temperature, except for the GL band (2.4 eV). The GL band is usually seen at high excitation intensities and is characteristic of an internal transition. Pertaining to the unusual temperature dependence of the lifetime, the capture coefficient of the GL-related defect showed a strong temperature dependence which behaved very similarly to that of giant traps, or attractive centers in semiconductors with very large capture cross sections at low temperatures. The increase in the lifetime of GL with increasing temperature can be explained if the optically created excited state of the C_N defect, which presumably causes the GL, acts like a giant trap, and internal transitions from this giant-trap-like excited state to the ground state, 0/+ level of the C_N defect produce GL. The measured PL lifetime of the GL is a sum of the lifetime of electron capture by the giant trap and the lifetime of the internal transition. This is the first observation of an optically generated giant trap.

The UVL and BL bands in Mg-doped GaN grown by HVPE were studied by varying the excitation intensity and temperature, and by using time-resolved studies. The position of the UVL (3.2 eV) peak blue-shifts with increasing excitation intensity, which can be explained by the presence of potential fluctuations. The BL peak (2.8 eV) also blue-shifts with increasing excitation intensity, and red-shifts as a function of temperature. These shifts can be explained by the transitions originating from a deep-donor to the Mg_{Ga} acceptor, and the corresponding donor-acceptor pair nature. This may be deduced since with increasing temperature, the BL peak

redshifts, signifying the thermal emission of close pairs, and the remaining contribution resulting from distant pairs.

Many unsolved puzzles regarding defect-related luminescence remain. For undoped GaN samples, the origins of the RL, YL, and GL have been speculated but much uncertainty remains. Additionally, multiple types of luminescence are in close proximity to each other for the RL and YL regions, and each well-resolved band must have a distinct origin. Interestingly, some of these bands may be related to each other by first and second charge states of the same defect. By performing careful excitation intensity and temperature dependent measurements, the correlation between bands can be shown.

Further mysteries remain for the Mg-doped GaN samples which depending on doping levels show the UVL and BL bands. Interesting behavior includes the peak shift of both the UVL and BL bands with temperature and excitation intensity, bleaching of the BL band, an interesting correlation between lifetime and ATQ, and hysteresis in the thermal quenching.

Defects in GaN may also be studied by uniaxial stress measurements where the samples are immersed in liquid helium, stress is applied, and the defect-related luminescence is measured. This rare and unexplored technique may shed light on the origin of defects. Data obtained from PL measurements should be compared with data obtained from secondary ion mass spectroscopy, positron annihilation spectroscopy, deep level transient spectroscopy and electron paramagnetic resonance measurements to gain deeper insight on the microscopic origins and properties of the point defects in GaN.

List of References

List of References

[1] S. Vandenkooy, *Finals Week - Spoken Word by Stefan Vandenkooy.* Accessed online: 22 April 2016. vimeo.com/128292930, (2015).

[2] B. Monemar, *Phys. Rev. B* **10**, 676 (1974).

[3] M. A. Reshchikov, A. Kvasov, T. McMullen, M. F. Bishop, A. Usikov, V. Soukhoveev, and V. A. Dmitriev, Phys. Rev. B **84**, 075212 (2011).

[4] M. A. Reshchikov, M. A. Foussekis, J. D. McNamara, A. Behrends, A. Bakin, and A.Waag, J. Appl. Phys. **111**, 073106 (2012).

[5] M. A. Reshchikov and H. Morkoc. *J. Appl. Phys.* **97**, 061301 (2005).

[6] M. A. Reshchikov, J. D. McNamara, A. Usikov, H. Helava, and Yu. Makarov, *Mater. Res. Soc. Proc.* **1736**, t05-05 (2014).

[7] M. A. Reshchikov, *Point defects in GaN, in Semiconductors and Semimetals: Defects in Semiconductors*, Editors: C. Jagadish, V. Privitera, and L. Romano, Vol. 91, Burlington, UK: Academic Press, 2015, pp. 315-367. ISBN: 978-0-12-801935-1

[8] M. A. Reshchikov, D. O. Demchenko, A. Usikov, H. Helava, and Yu. Makarov, *Proc. of SPIE-The International Society for Optical Engineering*, **9363**, 93630L (1-7) (2015).

[9] W. Shockley and J. W. T. Read, *Phys. Rev.* **87**, 835 (1952).

[10] V. N. Abakumov, V. I. Perel, and I. N. Yassievich, *Nonradiative recombinations in Semiconductors* (Elsevier, Amsterdam, 1991).

[11] M. A. Reshchikov, *J. Appl. Phys.***115**, 103503 (2014).

[12] M. A. Reshchikov, and R. Y. Korotkov, *Phys. Rev. B* **64** 115205 (2001).

[13] F. E. Williams, *J. Chem. Phys*. **19**(4), 457 (1951).

[14] F. Seitz, *Trans. Faraday Soc*. **35**, 74 (1939).

[15] D. L. Dexter, C. C. Klick and G. A. Russel, *Phys. Rev*. **100**(2), 603 (1955).

[16] C. C. Klick and J. H. Schulman, *Solid State Phys*. **5**, 97 (1957).

[17] K. K. Rebane, *Impurity Spectra of Solids* (Plenum, New York, 1970).

[18] A. M. Stoneham, *Theory of Defects in Solids* (Clarendon, Oxford, 1957).

[19] M. A. Reshchikov, D. O. Demchenko, J. D. McNamara, S. Fernandez-Garrido, and R. Calarco, *Phys. Rev. B* **90**, 035207 (2014).

[20] M. A. Reshchikov, A. J. Olsen, M. F. Bishop, T. McMullen, Phys. Rev. B 88, 075204 (2013).

[21] C. Díaz-Guerra, J. Piqueras, and A. Cavallini, *Appl. Phy. Lett*. **82**(13), 2050 (2003).

[22] D. M. Hofmann, D. Kovalev, G. Steude, B. K. Meyer, A. Hoffmann, L. Eckey, R. Heitz, T. Detchprom, H. Amano, and I. Akasaki, *Phys. Rev. B* **52**(23), 702 (1995).

[23] J. Mickevicius, G. Tamulaitus, P. Vitta, A. Zukauskas, M. S. Shur, J. Zhang, J. Yang, and R. Gaska, *Solid State Comm.* **145**, 312 (2008).

[24] S. F. Chichibu, K. Hazu, Y. Ishikawa, M. Tashiro, H. Namita, S. Nagao, K. Fujito, and A. Uedono, *J. Appl. Phys.* **111**, 103518 (2012).

[25] Y. Kawakami, K. Omae, A. Kaneta, K. Okamoto, T. Izumi, S. Saijou, K. Inoue, Y. Narukawa, T. Mukai, and SG. Fujita, *Phys. Stat. Sol.* (a) 183, 41 (2001).

[26] R. Dingle, and M. Ilegems, *Sol. Stat. Comm.* **9**, 175, (1971).

[27] P. Bergman, Gao Ying, B. Monemar, and P. O. Holtz, *J. Appl. Phys.* **61**(9), 4589 (1987).

[28] Y. -H. Kwon, S. K. Shee, G. H. Gainer, G. H. Park, S. J. Hwang, and J. J. Song, Appl. Phys. Lett. 76, 840 (2000).

[29] D. G. Thomas, J. J. Hopfield, and W. M. Augustyniak, *Phys. Rev.* **140**, 202 (1965).

[30] V. Yu Nekrasov, L. V. Belyakov, O. M. Sreseli, and N. N. Zinov'ev, *Semicondcutors* **33**(12), 1285 (1999).

[31] M. A. Reshchikov, G.-C. Yi, and B. W. Wessels, *Phys. Rev. B* **59**(20), 176 (1999).

[32] F. Shahedipour, and B. W. Wessels, *MRS Internet J. Nitride Semicond. Res*. **6**, 12 (2001).

[33] A. P. Levanyuk and V. V. Osipov, Usp. Fiz. Nauk **133**, 427 (1981) [Sov. Phys. Semicond. **3**, 1496 (1970)].

[34] S. Strauf, S. M. Ulrich, P. Michler, J. Gutowski, T. Böttcher, S. Figge, S. Einfeldt, and D. Hommel, Phys. Stat. Sol. B **228**, 379 (2001).

[35] H. Haag, B. Hönerlage, O. Briot, and R. L. Aulombard, *Phys. Rev. B* **60**, 11624 (1999).

[36] M. Godlewski et al., *Mater. Sci. Forum* **258-263**, 1149 (1997).

[37] R. Y. Korotkov, M. A. Reshchikov, and B. W. Wessels, *Physica B* **325**, 1 (2003).

[38] D. G. Chtchekine et al., *J. Appl. Phys*. **81**, 2197 (1997).

[39] R. Setiz, C. Gaspar, T. Monteiro, E. Pereira, M. Leroux, B. Beamont, and P. Gibart, *MRS Internet J. Nitride Semicond. Res.* **2**, 36 (1997).

[40] R. Y. Korotkov, M. A. Reshchikov, and B. W. Wessels, *Physica B* **273**, 80 (1999).

[41] M. A. Reshchikov, H. Morkoç, S. S. Park, and K. Y. Lee, *Appl. Phys. Lett*. **78**, 3041 (2001).

[42] M. A. Reshchikov, H. Morkoç, S. S. Park, and K. Y. Lee, *Appl. Phys. Lett*. **81**, 4970 (2002).

[43] R. Seitz, C. Gaspar, T. Monteiro, E. Pereira, M. Leroux. B. Beaumont, and P. Gibart. *J. Cryst. Growt.* **189/190**, 546 (1998).

[44] E. M. Goldys, M. Godlewski, R. Langer, A. Barski, P. Bergman, and B. Monemar. *Phys. Rev. B*. **60(8)**, 5464 (1999).

[45] B. Gil, A. Morel, T. Taliercio, P. Lefebvre, C. T. Foxon, I. Harrison, A. J. Winser, and S. V. Novikov, *Appl. Phys. Lett*. **79**, 69 (2001).

[46] G. Pozina, I. Ivanov, B. Monemar, J. V. Thordson, and T. G. Andersson, *J. Appl. Phys.***84**, 3830 (1998).

[47] C. G. Van de Walle, and J. Neugebauer, *Appl. Phys. Lett*. **76**, 1009 (2000).

[48] T. Sauncy, C. P. Palsule, M. Holtz, S. Gangopadhyay, and S. Massie, Phys. Rev. B 53, 1900 (1996).

[49] E. W. Williams, *Phys. Rev.* **168**(3), 168 (1968).

[50] K. D. Glinchuk, A V. Prokhorovich, and V. E. Rodionov, *Sov. Phys. Semicond.* **11**(1), 18 (1977).

[51] R. W. Gurney, and N. F. Mott, Trans. Faraday Soc. **35**, 69 (1939).

[52] M. A. Reshchikov, A. Usikov, H. Helava, and Yu. Makarov, *Appl. Phys. Lett.* **104**, 032103 (2014).

[53] M. A. Reshchikov, J. D. McNamara, F. Zhang, M. Monavarian, A. Usikov, H. Helava, Yu. Makarov, and H. Morkoç, "Zero-phonon line and fine structure of the yellow luminescence band in GaN", *Submitted to Phys. Rev. B in April 2016*.

[54] D. O. Demchenko, I. C. Diallo, and M. A. Reshchikov, *J. Appl. Phys.* **119**, 035702 (2016).

[55] M. A. Reshchikov, A. Usikov, H. Helava, and Yu. Makarov, *J. Electr. Mat.*, **44**(5), 1281 (2015).

[56] E. H. Hall, "On a New Action of the Magnet on Electric Currents." *American Journal of Mathematics*, **2**(3), 287–292 (1879).

[57] D. C. Look, *Characterization of GaAs Materials and Devices* (Wiley, New York, 1989). App. B.

[58] D. C. Look and R. J. Molnar, Appl. Phys. Lett. **70**, 3377 (1997).

[59] J. D. McNamara, M. Foussekis, H. Liu, H. Morkoç, M. A. Reshchikov, and A. A. Baski, *Proc. SPIE* **8262**, 826213 (2012).

[60] M. A. Reshchikov, J. D. McNamara, A. Usikov, H. Helava, and Yu. Makarov, *Phys. Rev. B* **93**, 081202(R) (2016).

[61] M. Lax, *Phys. Rev.* **119**, 1502 (1960).

[62] M. Lax, *J. Phys. Chem. Solids* **8**, 66 (1959).

[63] S. A. Kaufman, K. M. Kulikov, and N. P. Likhtman, *Fiz. Tekh. Poluprovodn*. **4**, 129 (1970) [*Sov. Phys. Semicond*. **4**, 102 (1970)].

[64] Akasaki and H. Amano, *J. Electrochem. Soc*. **141**, 2266 (1994).

[65] W. Götz, N. M. Johnson, J. Walker, D. P. Bour, and R. A. Street, *Appl. Phys. Lett*. **68**, 667 (1996).

[66] P. Kozodoy, H. Xing, S. P. DenBaars, U. K. Mishra, A. Saxler, R. Perrin, S. Elhamri, and W. C. Mitchel, *J. Appl. Phys.* **87**, 1832 (2000).

[67] H. Harima, T. Inoue, S. Nakashima, M. Ishida, and M. Taneya, *Appl. Phys. Lett*. **75**, 1383 (1999).

[68] S. M. Myers, A. F. Wright, G. A. Petersen, W. R. Wampler, C. H. Seager, M. H. Crawford, and J. Han, *J. Appl. Phys*. **89**, 3195 (2001).

[69] C. G. Van de Walle, Phys. Rev. B 56, R10020 (1997).

[70] H. Obloh, K. H. Bachem, U. Kaufmann, M. Kunzer, M. Maier, A. Ramakrishnan, and P. Schlotter, *J. Cryst. Growth* **195**, 270 (1998).

[71] U. Kaufmann, M. Kunzer, M. Maier, H. Obloh, A. Ramakrishnan, B. Santic, and P. Schlotter, *Appl. Phys. Lett*. **72**, 1326 (1998).

[72] H. Obloh, K. H. Bachem, U. Kaufmann, M. Kunzer, M. Maier, A. Ramakrishnan, and P. Schlotter, *J. Cryst. Growth* **195**, 270 (1998).

[73] J. M. Myoung, K. H. Shim, C. Kim, O. Gluschenkov, K. Kim, S. Kim, D. A. Turnbull, and S. G. Bishop, *Appl. Phys. Lett*. **69**, 2722 (1996).

[74] J. K. Sheu, Y. K. Su, G. C. Chi, B. J. Pong, C. Y. Chen, C. N. Huang, and W. C. Chen, *J. Appl. Phys*. **84**, 4590 (1998).

[75] E. Oh, H. Park, and Y. Park, *Appl. Phys. Lett*. **72**, 70 (1998).

[76] M. Smith et al., *Appl. Phys. Lett*. **68**, 1883 (1996).

[77] Y. Koide, D. E. Walker, Jr., B. D. White, L. J. Brillson, M. Murakami, S. Kamiyama, H. Amano, and I. Akasaki, *J. Appl. Phys*. **92**, 3657 (2002).

[78] E. Zacks, and A. Halperin, *Phys. Rev. B*, **6**(8), 3072 (1972).

[79] F. E. Williams, *J. Phys. Chem. Solids*, **12**, 265 (1960).

Vita

Joy Dorene McNamara was born in Newport News, Virginia on December 16, 1988. She received her Bachelor of Science in Physics in 2011 from Virginia Commonwealth University (VCU), and graduated Magna Cum Laude with University Honors, and a minor in Mathematics. In May 2013, she received the degree of Master of Science in Applied Physics. She began her doctoral studies in the VCU Nanoscience and Nanotechnology program in 2013, and completed her dissertation in the Spring of 2016. Joy worked under the supervision of Prof. Dr. Michael Reshchikov and Prof. Dr. Alison Baski, with a research focus on material characterization using Photoluminescence, Atomic Force Microscopy, and Kelvin probe techniques to study the surface and bulk properties of wide-bandgap semiconductors and their point defects.

Publications

M. A. Reshchikov, J. D. McNamara, F. Zhang, M. Monavarian, A. Usikov, H. Helava, Yu. Makarov, and H. Morkoç, "Zero-phonon line and fine structure of the yellow luminescence band in GaN", *Submitted to Phys. Rev. B in April 2016*.

M. A. Reshchikov, J. D. McNamara, A. Usikov, H. Helava, and Yu. Makarov. *Phys. Rev. B* **93**, 081202(R) (2016). "Optically generated giant traps in high-purity GaN"

M. A. Reshchikov, J. D. McNamara, A. Usikov, H. Helava, and Yu. Makarov. *Mater. Res. Soc. Proc.* **1736** (2015). "HVPE GaN with Low Concentration of Point Defects for Power Electronics"

M. A. Reshchikov, D. O. Demchenko, J. D. McNamara, S. Fernández-Garrido, and R. Calarco. *Phys. Rev. B* 90, 035207 (2014). "Green luminescence in Mg-doped GaN"

Joy D. McNamara, Michael Foussekis, Alison A. Baski, and Michael A. Reshchikov. *J. Vac. Sci. Tech. B* 32, 011209 (2014). “Low-temperature surface photovoltage in p-type GaN”

J. D. McNamara, A. Behrends, M. S. Mohajerani, A. Bakin, A. Waag, A. A. Baski, and M. A. Reshchikov. *AIP Conference Proceedings* 1583, 287 (2014). “Surface photovoltage in heavily doped GaN:Si,Zn”

M. A. Reshchikov, J. D. McNamara, and F. Shahedipour-Sandvik. *Phys. Stat. Sol. C*, 1–4 (2014). “Tunable thermal quenching of photoluminescence in GaN”

J. D. McNamara, A. A. Baski, and M. A. Reshchikov. *Phys. Stat. Sol. C*, 1–4 (2014). “Temperature-dependent Kelvin probe studies on GaN from 80 to 600 K”

M. A. Reshchikov, J. D. McNamara, S. Fernandez-Garrido, and R. Calarco. *Phys. Rev. B* 87, 115205 (2013). “Tunable thermal quenching of photoluminescence in Mg-doped p-type GaN”

M. A. Reshchikov, J. D. McNamara, A. Behrends, M. S. Mohajerani, A. Bakin, and A. Waag. *Phys. Stat. Sol. C* 10, No. 3, 507–510 (2013). “Higher than 90% internal quantum efficiency of photoluminescence in GaN:Si,Zn”

J. D. McNamara, M. Foussekis, A.A. Baski, X. Li, V. Avrutin, H. Morkoç, J.H. Leach, T. Paskova, K. Udwary, E. Preble, and M.A. Reshchikov. *Phys. Stat. Sol. C* 10, No. 3, 536–539 (2013). “Electrical and optical properties of bulk GaN substrates studied by Kelvin probe and photoluminescence”

Michael Foussekis, Josephus D. Ferguson, Joy D. McNamara, Alison A. Baski, and Michael A. Reshchikov. *J. Vac. Sci. Tech. B* 30, 051210 (2012). “Effects of polarity and surface treatment on Ga- and N-polar bulk GaN”

M. Foussekis, J. D. McNamara, A. A. Baski, and M. A. Reshchikov. *Appl. Phys. Lett*. **101**, 082104 (2012). “Temperature-dependent Kelvin probe measurements of band bending in *p*-type GaN”

M. A. Reshchikov, M. Foussekis, J. D. McNamara, A. A. Behrends, A. Bakin, and A. Waag. *J. Appl. Phys*. 111, 073106 (2012). “Determination of the absolute internal quantum efficiency of photoluminescence in GaN co-doped with Si and Zn”

J. D. McNamara, M. Foussekis, H. Liu, H. Morkoç, M. A. Reshchikov, and A. A. Baski. Gallium Nitride Materials and Devices VI, *Proc. of SPIE* 8262, (2012). “Temperature Dependent Behavior of the SPV for n-type GaN”

J. D. McNamara, J.D. Ferguson, M. Foussekis, I. Ruchala, M.A. Reshchikov, A.A. Baski, H. Liu, V. Avrutin, and H. Morkoç. *Mat. Res. Soc. Proc.* 1315, (2011). “Surface Characterization of Ga-doped ZnO layers”